

SYNTHESIS AND REACTIVITY
OF
ENEDIYNES

A Thesis

Presented to

The Faculty of Graduate Studies

of

Lakehead University

by

TIFFANY R. HECNAR

In partial fulfilment of requirements

for the degree of

Master of Science

February 19, 2004

© Tiffany Hecnar, 2004



Library and
Archives Canada

Bibliothèque et
Archives Canada

Published Heritage
Branch

Direction du
Patrimoine de l'édition

395 Wellington Street
Ottawa ON K1A 0N4
Canada

395, rue Wellington
Ottawa ON K1A 0N4
Canada

Your file *Votre référence*
ISBN: 0-612-96992-4
Our file *Notre référence*
ISBN: 0-612-96992-4

The author has granted a non-exclusive license allowing the Library and Archives Canada to reproduce, loan, distribute or sell copies of this thesis in microform, paper or electronic formats.

L'auteur a accordé une licence non exclusive permettant à la Bibliothèque et Archives Canada de reproduire, prêter, distribuer ou vendre des copies de cette thèse sous la forme de microfiche/film, de reproduction sur papier ou sur format électronique.

The author retains ownership of the copyright in this thesis. Neither the thesis nor substantial extracts from it may be printed or otherwise reproduced without the author's permission.

L'auteur conserve la propriété du droit d'auteur qui protège cette thèse. Ni la thèse ni des extraits substantiels de celle-ci ne doivent être imprimés ou autrement reproduits sans son autorisation.

In compliance with the Canadian Privacy Act some supporting forms may have been removed from this thesis.

Conformément à la loi canadienne sur la protection de la vie privée, quelques formulaires secondaires ont été enlevés de cette thèse.

While these forms may be included in the document page count, their removal does not represent any loss of content from the thesis.

Bien que ces formulaires aient inclus dans la pagination, il n'y aura aucun contenu manquant.

Canada

ABSTRACT
Synthesis and Reactivity
of
Enediynes

Tiffany Hecnar
Lakehead University

Supervisor:
Dr. Christine Gottardo

The discovery of a class natural products with anti-cancer properties, the enediynes, has stimulated interest in their research. Due to their cytotoxicity, these compounds are not feasible for use in cancer treatment, however, synthetic work has centered around improved stability, reduced toxicity and elucidation of the mechanism of the Bergman cyclization reaction. Protocols utilizing palladium-catalysed cross coupling reactions have been used extensively in the synthesis of enediyne analogues. Little work to date has investigated the effect of heteroatoms on the success of coupling reactions, thermal Bergman cyclizations and photochemically induced cyclizations. In this thesis, a synthetic study involving the coupling reactions of nitrogenous aromatic halides, halotriflates and a series of alkynes will be presented. Several enediyne analogues were synthesized in moderate to high yields, isolated and characterized. In general, it was observed that nitrogen heteroatoms increase the reactivity toward Sonogashira coupling reactions. In order to examine the effect of resonance and inductive effects on the reactivity under Sonogashira conditions, a series of competitive reactions between *m*- or *p*-substituted aryl iodides and iodobenzene were performed. In general, electron withdrawing substituents in the *m*- and *p*-positions increased the reactivity, while electron

donating substituents decreased it. It was observed that resonance effects have a larger effect on reactivity than inductive effects. Thermal and photochemical cyclization studies were performed for the nitrogenous aromatic enediynes synthesized. None of the enediynes were observed to cyclize thermally, while only the TMS- and phenyl-substituted enediynes were observed to photochemically cyclize.

ACKNOWLEDGEMENTS

I wish to thank Dr. Christine Gottardo for accepting me into her research group and providing guidance, support and encouragement throughout my graduate studies. Without her assistance, insights and direction, this thesis would not have been completed. I thank my committee members, Dr. Jeff Banks, Dr. Craig MacKinnon, and Dr. Greg Spivak for their generosity and insights. I also thank Debbie Leach and Ainsley Bharath for all of their assistance and training. I am also grateful to Ain Raitasak and Keith Pringnitz for their patience and guidance on GC-MS, IR and NMR instrumentation. Finally, I thank my friends and family for all of the patience and love they have shown me during my studies.

LIST OF ABBREVIATIONS

DNA	Deoxyribonucleic Acid
ED	Electron Donating
Et	Ethyl
EW	Electron Withdrawing
FTIR	Fourier Transform Infrared
GC-MS	Gas Chromatography Mass-Spectrometry
GLC	Gas Liquid Chromatography
HPLC	High Performance Liquid Chromatography
IR	Infrared
OAc	Acetate
Me	Methyl
NMR	Nuclear Magnetic Resonance
THF	Tetrahydrofuran
TLC	Thin Layer Chromatography
TIPS	Triisopropylsilyl
TMS	Trimethylsilyl
AU	Atomic Units

TABLE OF CONTENTS

	PAGE
ABSTRACT	i
ACKNOWLEDGEMENTS.....	iii
LIST OF ABBREVIATIONS.....	iv
LIST OF TABLES.....	viii
CHAPTER ONE: A REVIEW OF ENEDIYNE STRUCTURE AND REACTIVITY	
1.1 <u>Introduction</u>	1
1.2 <u>Classes of Naturally Occurring Eneidyne</u>	1
1.2.1 Mode of Action.....	4
1.2.2 Thermal Bergman Cyclizations.....	5
1.2.3 Photochemical Bergman Cyclizations.....	10
1.2.4 Synthesis and Applications of Eneidyne.....	14
CHAPTER TWO: SYNTHETIC AND REACTIVITY STUDIES INVOLVING SONOGASHIRA COUPLING REACTIONS	
2.1 <u>Introduction</u>	16
2.1.1 Stephens-Castro Coupling.....	16
2.1.2 Sonogashira Coupling.....	17
2.1.3 Coupling By Thorand and Krause.....	19
2.2 <u>Synthesis of Nitrogenous Aromatic Eneidyne</u>	20
2.2.1 Synthetic Study of Nitrogenous Alkynyl Aromatics Using Sonogashira Coupling.....	21

2.3 <u>Results and Discussion - Nitrogenous Aromatic Eneidyne</u>	22
2.3.1 Sonogashira Coupling Percent Yield Trends.....	24
2.4 <u>Reactivity Study of <i>meta</i>- and <i>para</i>-substituted iodobenzenes</u>	30
2.4.1 Competition Reactions of <i>meta</i> - and <i>para</i> -substituted iodobenzenes.....	30
2.4.2 Relative Reactivities for the Competitive Coupling Study.....	31
2.4.3 Conclusion.....	39

CHAPTER THREE: A SYNTHETIC STUDY INVOLVING THE BERGMAN
CYCLIZATION

3.1 <u>Introduction</u>	41
3.1.1 Thermal Bergman Cyclization.....	41
3.1.2 Photochemical Bergman Cyclization.....	43
3.2 <u>Cyclizations of Nitrogenous Aromatic Eneidyne</u>	44
3.3 <u>Results and Discussion</u>	45
3.3.1 Percent Yield Trends.....	49
3.3.2 Conclusion.....	54

CHAPTER FOUR: EXPERIMENTAL

4.1 <u>General Experimental Techniques, Instrumentation and Materials</u>	56
4.2 <u>Preparations</u>	59
4.2.1 Procedures for the Preparation of Starting Materials.....	59
4.2.2 Procedures for Sonogashira Coupling Reactions.....	64
4.2.3 Procedures for Alkynyl Deprotections.....	70

4.2.4 Procedures for Thermal Cyclizations.....	71
4.2.5 Procedures for Photochemical Cyclizations.....	73
4.2.6 Procedures for Competitive Rate Reactions.....	75
APPENDIX	79
REFERENCES.....	83

LIST OF TABLES

	PAGE
TABLE ONE: Isolated Yields for Sonogashira Coupling Reactions.....	27
TABLE TWO: Concentration Ratios for Competitive Rate Reactions Between <i>meta</i> - and H-substituted Aryl Iodides.....	35
TABLE THREE: Concentration Ratios for Competitive Rate Reactions Between <i>para</i> - and H-substituted Aryl Iodides.....	37
TABLE FOUR: GC Yields for Cyclization Reactions.....	50
TABLE FIVE: Calculated <i>cd</i> for Synthesized Eneidyne.....	53
TABLE SIX: HPLC Separation Method for Iodoanilines.....	76
TABLE SEVEN: HPLC Separation Method for Iodoanisoles.....	76
TABLE EIGHT: HPLC Separation Method for Iodobenzotrifluorides.....	76
TABLE NINE: HPLC Separation Method for Iodoethylbenzene.....	77
TABLE TEN: HPLC Separation Method for Iodonitrobenzenes.....	77
TABLE ELEVEN: HPLC Separation Method for Iodophenols.....	77
TABLE TWELVE: HPLC Separation Method for Iodotoluenes.....	78
TABLE THIRTEEN: Competitive Rate Experiment Data for Iodoanilines versus Iodobenzene.....	79
TABLE FOURTEEN: Competitive Rate Experiment Data for Iodoanisoles versus Iodobenzene.....	79
TABLE FIFTEEN: Competitive Rate Experiment Data for Iodobenzotrifluorides versus Iodobenzene.....	80

TABLE SIXTEEN: Competitive Rate Experiment Data for Iodonitrobenzenes versus
Iodobenzene.....80

TABLE SEVENTEEN: Competitive Rate Experiment Data for Iodophenols versus
Iodobenzene.....81

TABLE EIGHTEEN: Competitive Rate Experiment Data for Iodotoluenes versus
Iodobenzene.....81

TABLE NINETEEN: Competitive Rate Experiment Data for 4- Iodoethylbenzene
versus Iodobenzene.....82

CHAPTER ONE

A REVIEW OF ENEDIYNE STRUCTURE AND REACTIVITY

1.1 Introduction

The discovery of natural products and their possible applications often spark intense research. In the mid 1980s, a class of compounds called the enediynes was isolated from bacterial sources. They were found to possess antibiotic and anticancer functions, and were considered as potential anticancer drugs. This activity was a result of their irreversible and selective DNA cleaving ability. Unfortunately, these compounds are highly toxic, and too unstable for clinical applications.^{1,2} Consequently, research has been directed towards design and synthesis of enediyne analogues that retain the selectivity and efficiency of the natural products, but are less toxic and more stable.^{2,3,4,5,6,7,8} A successful enediyne drug would possess a stable enediyne core that could be activated in a controlled manner, and be produced using a synthetically simple strategy.

1.2 Classes of Naturally Occurring Eneidyynes

Natural enediyne antitumour antibiotics possess a characteristic core, consisting of a conjugated (Z)-1,5-diyne-3-ene moiety, within the compound.^{2,9} Five classes of naturally occurring enediynes are known. Each class is structurally similar to the following five natural compounds (Figure 1):² calicheamicin, **1**, dynemicin, **2**, esperamicin, **3**, kedarcidin chromophore, **4**, and C-1027 chromophore, **5**. Similar reactivity is exhibited by the neocarzinostatin chromophore, **6**, upon activation (Figure 2).² Unlike the enediyne family, **6** contains an enyne-cumulene core.

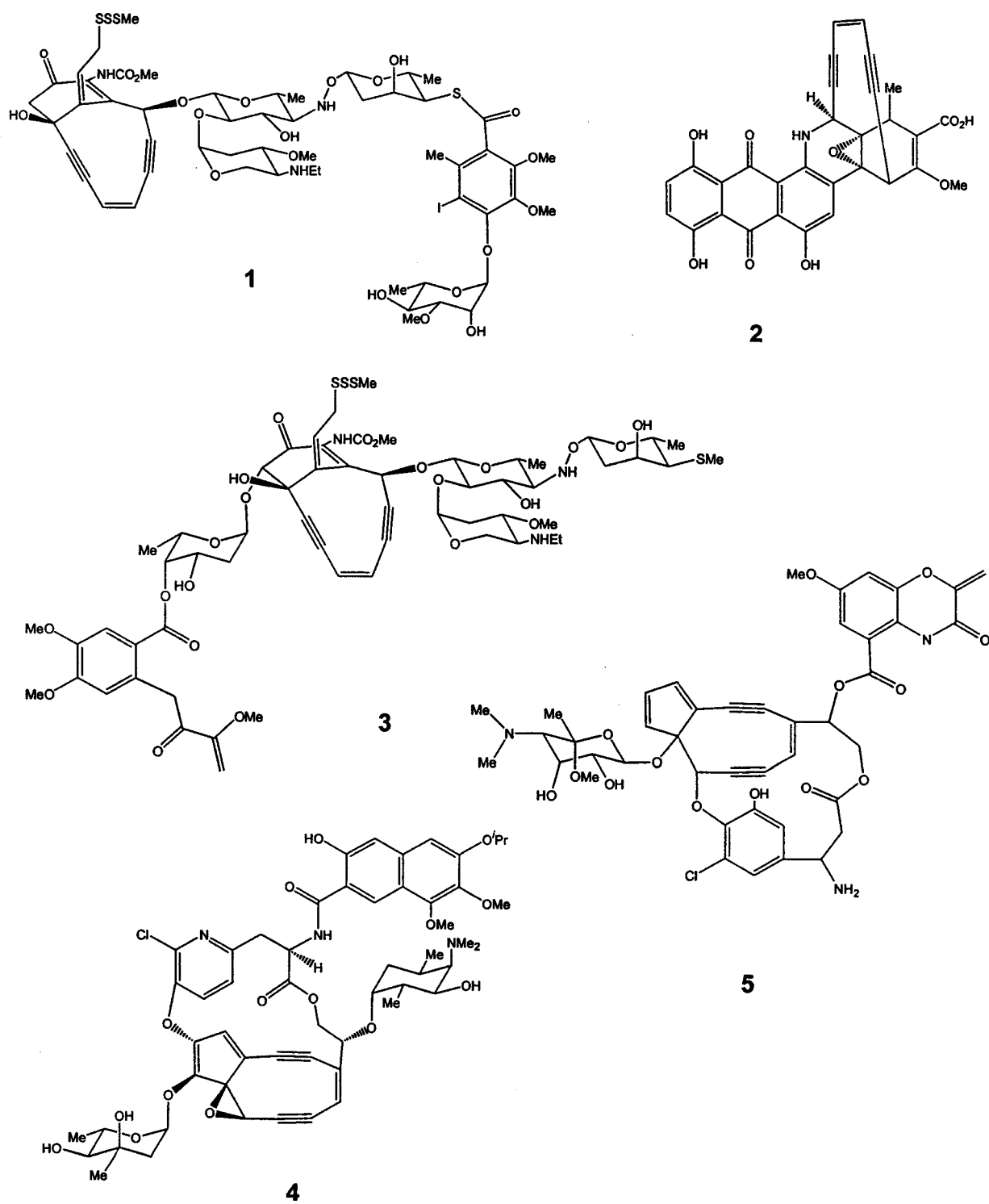
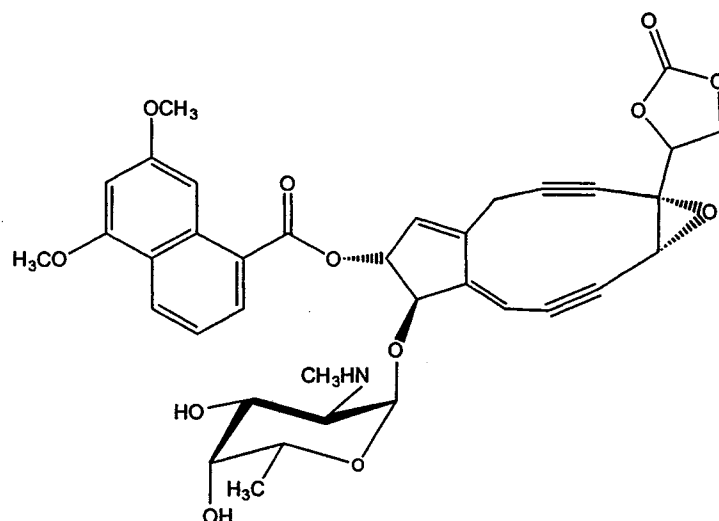


Figure 1²: Structures of enediyne natural products.



6

Figure 2²: Structure of neocarzinostatin.

In naturally occurring enediynes, the enediyne core is contained within a nine- or ten-membered ring.² Of the two ring sizes, only the ten membered rings are stable. Molecular components within the compound act to stabilize the enediyne until it has reached the target DNA and is biologically activated. The nine membered enediyne rings are not stable individually, and derive thermal stability from the non-covalent interactions via association with apoproteins. In addition, the apoprotein functions to direct the enediyne to the DNA target.^{2,10} Characteristically, enediynes contain three moieties that are essential to their function. Firstly, a delivery system ensures that the compound penetrates cellular membranes and intercalates between the minor grooves of the DNA. Secondly, a triggering device activates the highly strained diacetylenic ring system to perform the third function, a Bergman cyclization reaction.^{2,9} Activation can be triggered by bioreductions or isomerizations that can occur with light,¹¹ bases,¹² metal ions,¹³ or nucleophiles.^{1,14}

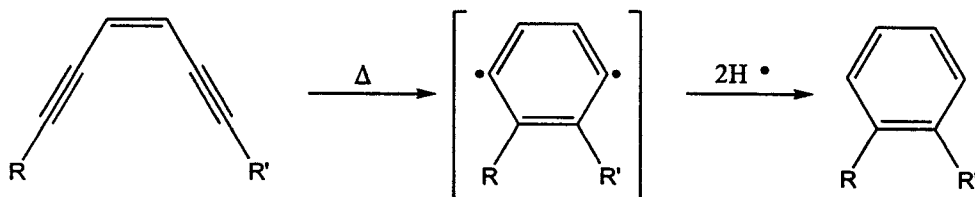
3

1.2.1 Mode of Action

Enediynes are interesting as potential drugs because they require activation before they are biologically active and, therefore, are considered prodrugs.^{2,5,15} Extremely potent anticancer antibiotics, natural product enediynes have been shown to be cytotoxic in concentrations as low as picomolar.¹⁶ Potentially this cytotoxicity can be minimized through drug design, so that a specific trigger is required and activation occurs only in designated cells. This would result in reduced cytotoxicity, and, thus, the toxic effects would not be seen in non-cancerous cells throughout the body.

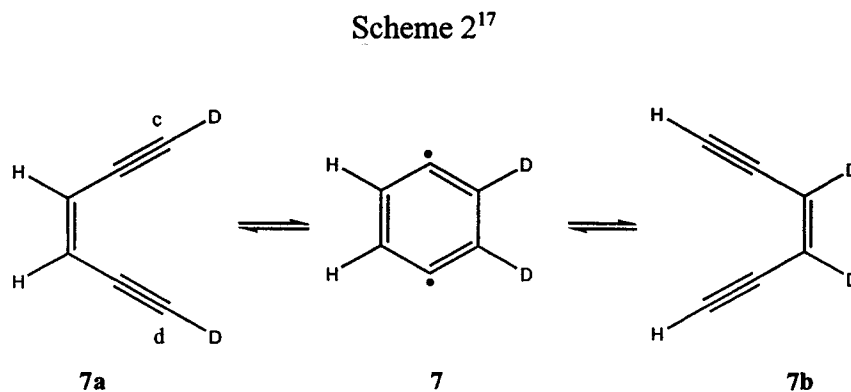
The mode of action is commonly accepted and, it is thought that DNA cleavage occurs in several stages.^{2, 9, 10} A structural feature of the compound is recognized and directed to the nucleus where planar portions of the enediyne drug intercalate in the minor groove of the DNA. Through a series of reactions, which depend on the identity of the trigger portion of the molecule, a conformational change in the enediyne moiety is induced and Bergman cyclization can occur (Scheme 1).^{2, 17, 18, 19, 20} The 1,4-benzenoid biradical that is generated abstracts two hydrogen atoms from the phosphate backbone of DNA and causes either double or single strand damage, and ultimately induces cell death.^{21, 22, 23}

Scheme 1²



1.2.2. Thermal Bergman Cyclizations

Remarkably, the 1,4-benzenoid biradical had been observed and studied fifteen years prior to the discovery and elucidation of natural product enediynes. Bergman *et al.* synthesized a 1,4-dehydrobenzene, **7**, employing a unimolecular isomerization reaction of *cis*-3-hexene-1,5-diyne with deuterium labels at the acetylenic positions, **7a** (Scheme 2).¹⁷ **7a** underwent deuterium scrambling rapidly at 200°C, and subsequent NMR showed an even distribution of deuterium between the acetylenic and vinylic positions. The results required that the intermediate species possessed a C₂ axis of symmetry. This strongly supported the proposed structure of **7** as an intermediate.¹⁷ Bergman trapped and characterized the proposed *para*-benzyne biradical intermediate by repeating the experiment in the presence of hydrogen donors, as shown in Scheme 1.



Much work has been completed to elucidate the factors that control the kinetics of the thermal Bergman cyclization. Two distinct theories have been proposed to explain the reactivity of enediynes. In an attempt to rationalise the reactivity of natural product enediynes, Nicolaou *et al.* examined a series of enediynes.²⁴ It was postulated that the reactivity towards Bergman

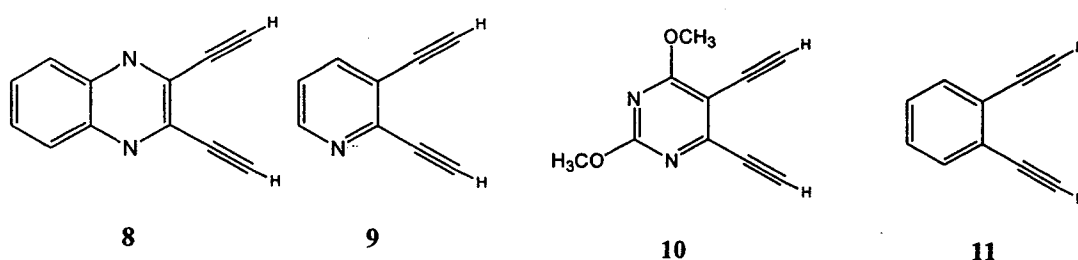
cyclization was determined by the distance calculated and observed between the acetylenic carbons (*cd*), Scheme 2. A correlation between their respective stabilities and the *cd* was observed. It was concluded that distances lower than 3.20 Å suffered spontaneous cyclization, and were termed transient intermediates (Scheme 2). Enediynes with *cd* between 3.20 and 3.31 Å cyclize at 25°C, while distances greater than 3.31 Å are known to be stable at 25°C. From this correlation it was concluded that enediyne thermal stability was a direct result of *cd* alone.

Nicolaou's conclusions have been discussed greatly, and criticized for their limitations. Further calculations by Snyder have indicated that although *cd* and reactivity are related in monocyclic systems, they do not apply consistently to more complex ring fused systems.²⁵ This was concluded upon examination of several sample systems. In related calculations, the transition state for cyclization was shown to possess 35% biradical character, lending support to Bergman's proposed mechanism. As a result, Snyder proposed that fusion of additional rings introduces competitive strain components that are not related to the diminished kinetic barriers enjoyed by shorter *cd* in monocyclic systems.²⁵

To support the previous work, Magnus *et al.* conducted kinetic studies on related enediynes to support the strain energy versus *cd*.²⁶ Consideration of the kinetic data obtained led to the conclusion that the cyclization rates of enediynes are governed by strain-energy modulation in the pseudocyclic transition state. From these extensive experimental determinations it was concluded that for fused ring systems, the rate of cyclization is influenced much more strongly by ring strain energy rather than the proximity of the acetylenic carbons. Other studies reinforce this conclusion, including an elegant comparison between computer modelled *cd*, rates and strain energy, and those determined by experiment, which found excellent correlation between

theoretical and experimental values.^{27,28}

Of the three factors believed to be involved in the activity of an enediyne towards Bergman cyclization, two (*cd* and strain energy) have been discussed. The third factor is broadly referred to as electronic effects. Several aspects of this category have been studied to date, including heteroatomic effects, solvent dependence, aryl ring substitutions, and acetylenic substitutions. In an attempt to elucidate how aromaticity and electronic factors influence the rate of cyclization, Kim *et al.* have synthesized several heteroatomic aromatic enediynes (**8-10**) and conducted some kinetic experiments.³² It had been previously determined that non-aromatic enediynes have shorter half-lives than arenediynes, however, the influence of the double bond has yet to be clarified.²⁹ The data indicated that the position of electron-withdrawing substituents associated with the double bond appear to facilitate Bergman cyclization.^{30,31}



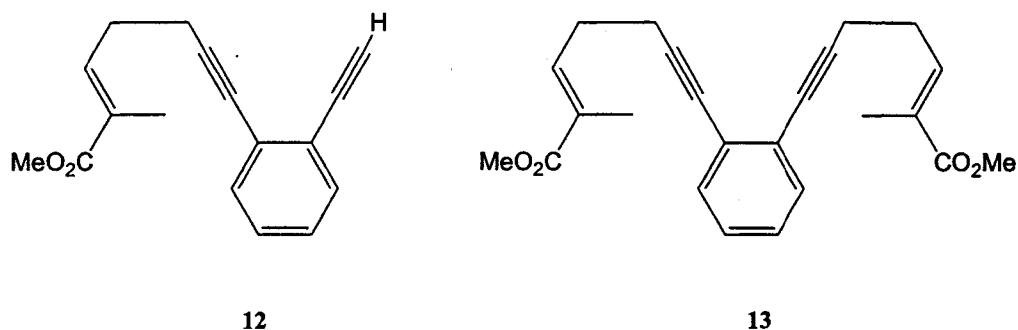
Enediynes **8-10** were synthesized, their kinetics of cyclization measured and their respective activation energies were calculated utilizing an Arrhenius relationship (rate of disappearance of enediyne versus time). The data obtained were compared to an analogous non-heteroaromatic enediyne, **11**. Compounds **9** and **10** were found to have decreased activation energies compared to compound **11**. Enediyne **10** was found to be the most reactive acyclic arenediyne studied to date. Addition of an aromatic ring in compound **8**, increased the activation

energy to greater than that of enediyne 11.³² During the course of these experiments, cyclized products were formed in better yields with less polar solvents, and the half-lives were found to correlate linearly with solvent dielectric constants and $E_T(30)$ values^{33,34}. This observation is intriguing because it has been reported that cyclization of similar enediynes is solvent independent. Although, requiring more study to examine whether this phenomenon is general for cyclizations, specific solvents could be utilized to enhance or suppress Bergman cyclization with respect to competing reactions.

Also under study is the effect of substitution on an arenediyne.³⁵ A series of 4-substituted-1,2-diethynylbenzenes were cyclized and kinetic experiments indicated a linear free energy relationship between rate of cyclization and the Hammett σ_m substituent coefficient. Manipulation of the electron withdrawing or electron releasing substituents can be utilized to affect the electronic nature of the double bond of the enediyne. In accordance with other studies, the enediyne with the most electron-withdrawing substituent, showed the shortest half-life, while those with electron releasing substituents had the longest half-lives. Most derivatives appeared to exhibit half-lives which corresponded with the nature of the electronic properties, except for the ketone and ester analogues, which exhibited the opposite trend. The data was plotted against various Hammett coefficients, where σ_m produced the best correlation with $\rho = 0.654$. The value of ρ was reasonable because the reaction is believed to proceed through uncharged transition states and intermediates. Development of Hammett relationships for the Bergman cyclization is extremely important since the reaction is unusual in its generation of a neutral σ,σ -biradical.

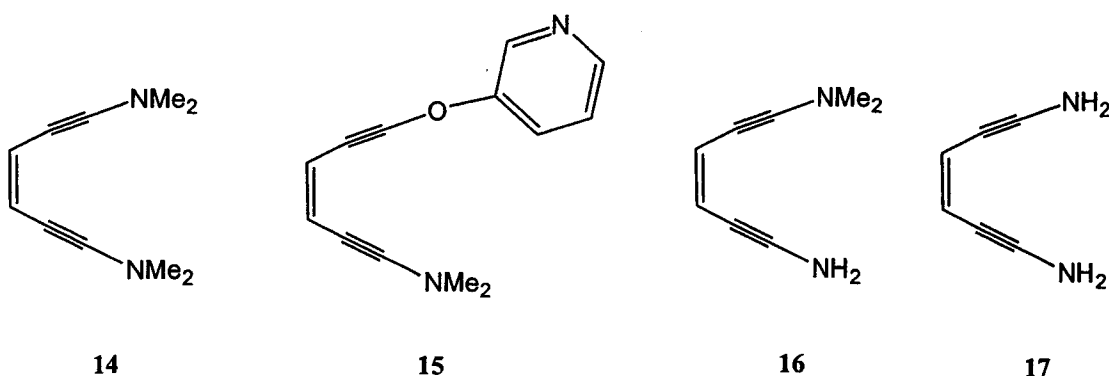
In contrast to the electronic effect of substitution of aryl rings, the substituent effect on the acetylenic carbons has received a great deal of study from experimental^{36,37} to computer

modelling,³⁸ and a combination of the two.³⁹ Grissom *et al.* examined the role of acetylenic tethers on the rate of Bergman cyclization of enediyne **11**.³⁶ Incorporation of the first tether, **12**, acted to slow the rate of cyclization moderately. In contrast, the incorporation of a second tether, **13**, slowed the rate considerably.³⁶



The dramatic steric effect of functional groups on the temperatures of Bergman cyclization is elegantly exhibited by the study of enediynes **14-17**. Enediyne **14** is thermally stable and cyclizes at a temperature of 186°C. Substitution of one dimethylamino group with 3-hydroxypyridine, **15**, significantly reduces the cyclization temperature to 149°C. This effect is suspected to be the influence of two factors. Firstly, the pyridine can rotate out of the enediyne plane about the oxygen, thus relieving steric interactions with the opposing substituent. Secondly, the insertion of the *sp*³ hybridized oxygen between the pyridine ring and the alkyne terminus increases the distance between the two and thereby reduces the effects of the substituent. An interesting trend is realized with enediynes **14**, **16** and **17**. Substitution of one of the dimethylamino groups for an amino group, **16**, dramatically reduces the cyclization temperature to 139°C. Substitution of the NMe₂ group to give **17**, resulted in a reduced cyclization temperature of 106°C. The enhanced thermal reactivity of **17** is a result of the reduced steric hindrance of the primary amine functionalities, in combination with intramolecular hydrogen bonding.³⁷ In an

attempt to describe only electronic effects, a comprehensive computer analysis of many acetylenic substituted enediynes has been completed. It indicated that strongly electron-withdrawing substituents increase the cyclization barrier, while σ -donating substituents decrease it and π conjugation, especially donation, has little effect.³⁸

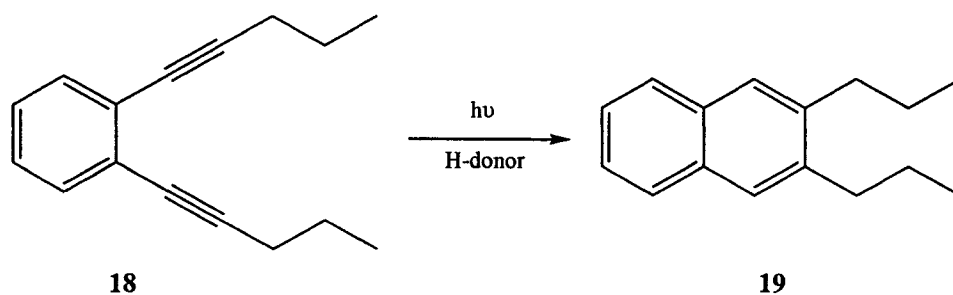


1.2.3 Photochemical Bergman Cyclizations

Of interest to synthetic chemists is the design of an enediyne drug that is thermally stable, but easily triggered *in vivo*. This has led to investigations into the feasibility of triggering the Bergman aromatisation with light. It has been proposed that biradicals (such as dehydroaromatics) can be photo-induced and exist as singlet or triplet states.¹⁴ Some molecules are raised to an excited singlet state through light absorption and deactivation can occur by fluorescence, intersystem crossing (spin flip) to a triplet state, and phosphorescence.⁴⁰ Assuming that a singlet or triplet excited state leads to a cyclized product, it is theoretically possible that Bergman cyclization could be triggered by light.

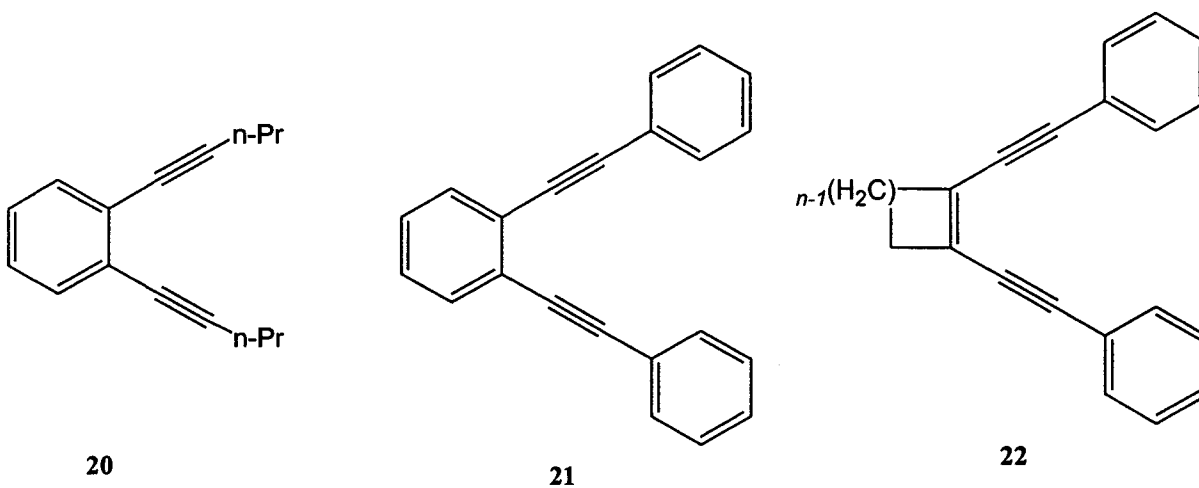
Proceeding with the notion of photochemical induction, Turro *et al.* photoirradiated 3-benzo-1,5-diyne **18** and isolated a Bergman type product, substituted naphthalene **19**.¹⁴

Mechanistic studies were completed utilizing a variety of triplet sensitizers, such as acetophenone, acetonaphthone and xanthone. In these studies, **19** was not observed in the presence of any triplet sensitizers, thus indicating that if a radical mechanism operated, then the intermediate was a singlet and not a triplet state. The products isolated from the irradiated solutions contained the Bergman product (where hydrogens had been abstracted) from a hydrogen donor, or a reduced alkyne. These observations were indicative of a radical mechanism, however, it was not the only possibility. It was observed that even when hydrogen donors were used in large excess in synthetic and thermal investigations of the Bergman thermal reaction, yields were moderate to poor, and polymerization was very competitive.¹⁴



Similar to the study of thermal cyclizations, some studies has been made of substitution of the acetylenic carbons, ring strain, and computational analysis of the transition states for photochemical Bergman cyclization, but not to the extent amassed for the thermal reactions. Some emphasis has been placed on elucidation of the nature of the transition state. Extensive computer modelling of cyclic enediynes also indicates that cyclization arises from an excited singlet state.⁴¹ In contrast to thermal reactions, photochemical cyclizations exhibit competing photoreduction reactions. The extent of the competition appears to be governed by the nature of the acetylenic substituents. Cyclization of enediyne **20** yields 25% of the cyclized product, as well

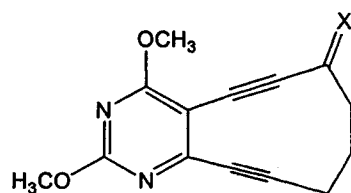
as three photoreduced products. In contrast, enediyne **21** yields only the Bergman product, and photoreduced products were not detected. When subjected to triplet sensitization, **21** fails to react. The failure of **21** to produce photoreduced products and react in triplet sensitization studies is rationalized by the proposal that the photochemical Bergman cyclization proceeds from a singlet excited state and photoreduced products arise from intersystem crossing to a triplet state. The failure of **21** to undergo intersystem crossing is a result of the phenyl rings forcing the enediyne into a more rigid conformation.¹⁴ Molecules with structural rigidity are expected to exhibit higher fluorescence quantum yields (excited singlet state to ground state relaxation process) than less rigid molecules. This hypothesis is supported by the lower fluorescence quantum yield of **20** as compared to **21**.¹¹



An inclusive examination of the effects of ring strain on photochemical cyclization has been completed. A series of analogues, **22**, was synthesized containing four- to eight- membered rings. The seven- and eight- membered rings showed lower conversion efficiency despite a considerable decrease in *cd*. This indicated that although *cd* may form a component of the reactivity of enediynes, it is ring strain energy that governs reactivity in the photochemical

reaction.⁴²

To date, only one examination has compared thermal and photochemical Bergman reactions directly.⁴³ Neither reaction is superior to the other in a generalized sense as the success of the photochemical reaction depends on the tendency for the enediyne to form excited triplet states (a competing process), and the success of the thermal reaction depends on thermal stability. For example, the alcohol substituted enediyne **23**, photochemically cyclized at 40°C with a yield of 80% and a half-life ($t_{1/2}$) of twenty-nine minutes for the starting material, while the thermal reaction was sluggish, $t_{1/2} = 58$ hr at 60°C. In contrast, ketone **24** in a photochemical reaction had a poor yield of 10% after irradiation for 2 hours, with 34% of the starting material remaining utilizing identical conditions as those stated above. The thermal reaction on the other hand exhibited a 92% yield when the reaction was performed at 80°C for 10 hours. The thermal product was irradiated and found to be stable, thus photodegradation was not a factor in the poor photochemical yield. The major difference in reactivity was believed to arise from the ketone's propensity to form triplet states that are prone to hydrogen and electron abstraction and not formation of the Bergman product.⁴³



23 X = H, OH⁴³
24 X = O

1.2.4. Synthesis and Applications of Eneidyne

Studies of Bergman cyclization rely on one's ability to prepare enediynes. Currently, new tools are being utilized in the design of enediynes, their synthesis, and their reactivity. Computer modelling is emerging as a tool to "test" enediyne drugs for desired properties, such as thermal stability, prior to chemical synthesis, and has produced favourable results.¹⁸ New methods for synthesis of enediynes are also being studied. The widespread approach uses a palladium coupling reaction between the alkyne and ene moieties.^{44,45,46} Nuss *et al.* have been utilizing the Norrish type II cleavage of an α,β -unsaturated carbonyl to form the desired enediyne.⁴⁷ Grissom *et al.* utilized tandem Bergman cyclization reactions to synthesize two and three fused ring systems simultaneously.^{48,49} Finally, different metal ions have been found to promote Bergman cyclization by lowering the activation barrier. To date, Cu(II), Zn(II) and Mg(II) have been used to promote cyclization, with a Mg(II) complexed enediyne cyclizing at room temperature.^{50, 51}

Although a great deal of evidence has been amassed to explain the reactivity and mechanism for both the thermal and photochemical reactions, much work has yet to be completed. Also, the effects governing the reactivity of enediynes towards cyclization must be investigated further and their trends identified and rationalized. Perhaps the most exciting aspect of the study of enediynes is the potential applications already imagined and those still to be discovered.

When designing an enediyne analogue for potential medical applications, several factors must be considered. Firstly, the enediyne must have a planar component that can intercalate with DNA. The analogue must also be thermally stable under physiological conditions, and exhibit very low or no general cytotoxicity. Activation of the analogue toward the Bergman cyclization

must be due to a specific, controllable trigger, for example, light. Finally, the analogue must be synthetically simple. This thesis investigates the synthesis of nitrogenous aromatic enediynes utilizing Sonogashira coupling. Chapter Two of this thesis presents a synthetic study of nitrogenous aromatic enediynes and a reactivity study of 1,3-substituted and 1,4-substituted iodobenzenes. Contained in this section is an examination of the influences of different nitrogenous aromatics, and alkynes and their effect on coupling. Chapter Three presents a synthetic study of thermally and photochemically induced Bergman cyclizations of nitrogenous enediynes synthesized in Chapter Two.

CHAPTER TWO

SYNTHETIC STUDY AND REACTIVITY STUDIES INVOLVING THE SONOGASHIRA COUPLING REACTION

2.1 Introduction

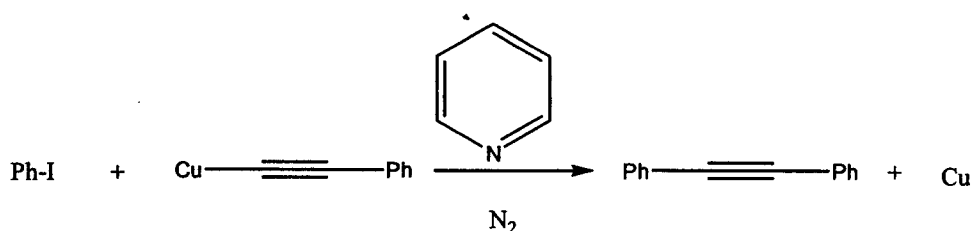
The synthesis of a potential enediyne analogue drug, requires an expedient and simplistic synthesis, preferably with a high yield. Routes to an enediyne core were discussed briefly in Chapter One. This chapter will focus on Sonogashira palladium cross-coupling reactions as a method of enediyne synthesis. A survey of the literature shows that many carbon-carbon coupling procedures require a metal catalyst.^{52, 53, 54, 55} Palladium is often the catalyst of choice when coupling *sp* and *sp*² carbon centres. Haloalkenes are most frequently used, however, some couplings have been achieved using sulfonate ester alkenes.^{44,46} This chapter presents the results of two different studies. The first study describes the synthesis of the nitrogenous aromatic enediynes while the second study is a reactivity study of *meta*- and *para*-substituted iodobenzenes.

2.1.1 Stephens-Castro Coupling

The first study of metal-mediated cross-coupling reactions was completed by Stephens and Castro in the early 1960s.⁵⁵ They studied the formation of enynes through the coupling of cuprous acetylides with aryl halides (Scheme 3).⁵⁵ They also studied the reactivity of *para*-substituted iodobenzenes towards coupling with cuprous phenyl acetylide. They found that electron withdrawing substituents, such as *p*-NO₂ reacted faster than *p*-H which in turn reacted

faster than electron releasing substituents, such as *p*-OCH₃. It was found that the reaction would not occur if the halogen (leaving group) was not bonded to an *sp*²-hybridized carbon. The order of reactivity exhibited in these studies was found to vary periodically down the halogen group, with iodides reacting the fastest. Fluoride starting materials did not react.

Scheme 3⁵⁵

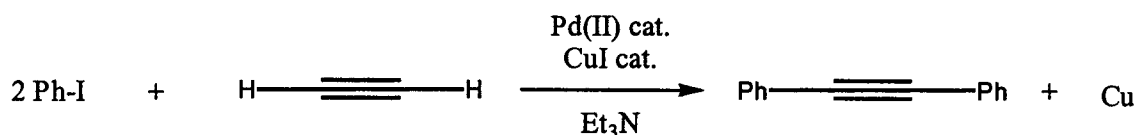


2.1.2. Sonogashira Coupling

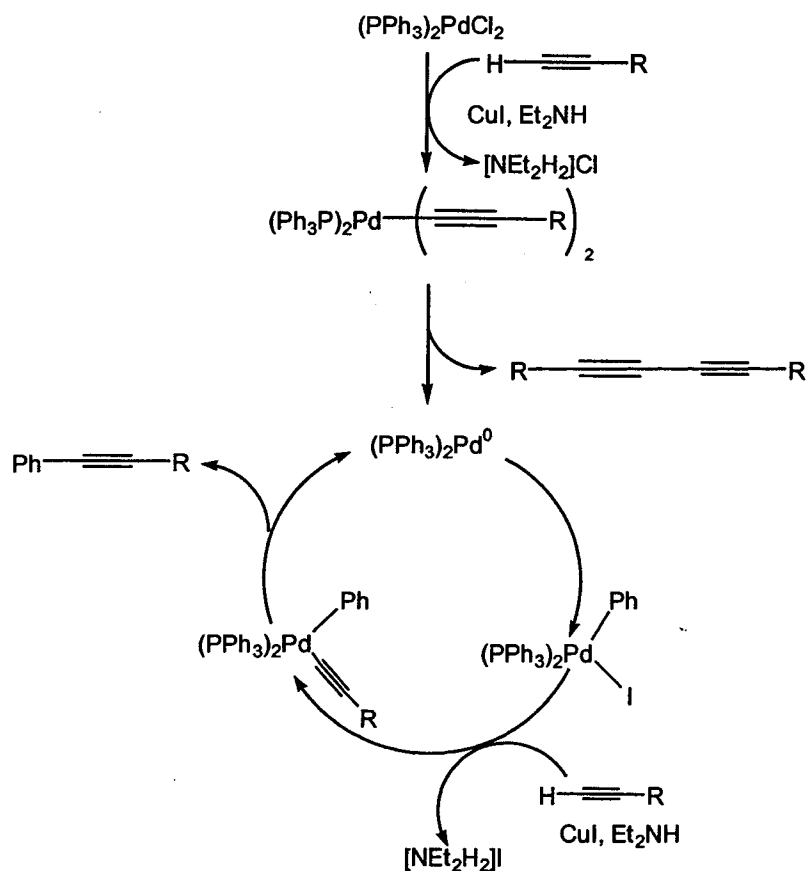
Although the Stephens-Castro coupling procedure was effective in the formation of the desired coupled product, the violent reactivity of the cuprous acetylides and the rigorous conditions required made a milder procedure desirable. The procedure was modified so that the cuprous acetylides were generated *in situ*. Bromoalkenes, iodoarenes and bromopyridines were coupled with acetylenes at room temperature using a Pd(II) catalyst and amine solvent (Scheme 4).⁵⁶ Although some modifications had been made, the efficiency of Sonogashira coupling of arylbromides and terminal alkynes was not ideal. Due to the low reactivity of the arylbromides, forcing conditions were required for the coupling to occur. To improve the reactivity, aryl iodides were used instead of arylbromides, in spite of their greater cost. The greater reactivity was a result of the more polarizable C-I bond which facilitated higher yields in coupling. In order to

obtain high yields, it was necessary to purify reagents prior to reaction and exclude oxygen. Large excesses of alkyne were required and it was found that when oxygen was allowed to enter the reaction vessel, Glaser or homocoupling of the alkyne was observed.² In addition to the expense of the alkyne, difficulties were encountered when attempting to isolate the homocoupled product from the desired products.

Scheme 4⁵⁶



In the proposed mechanism (Scheme 5),³³ the active catalyst is thought to be a Pd (0) species, therefore, the first step in the mechanism requires that the Pd(II) catalyst must be reduced. This reduction is achieved through the oxidative homocoupling of the alkyne and alkynylation of the Pd(II) catalyst. This process is catalysed by cuprous iodide in the presence of diethylamine. The Pd(0) catalyst that is generated enters the catalytic cycle and oxidatively adds an aryl or vinyl halide. The oxidative addition is followed by alkynylation of the adduct to yield the aryl or vinyl alkynyl complex of palladium. The coupled product is formed by reductive elimination, regenerating the Pd(0) catalyst. It was observed that the CuI was vital to the progress of the reaction, however, elucidation of its role was not investigated in this study. Further study by another group attempted to improve on the efficiency of the reaction.⁵³

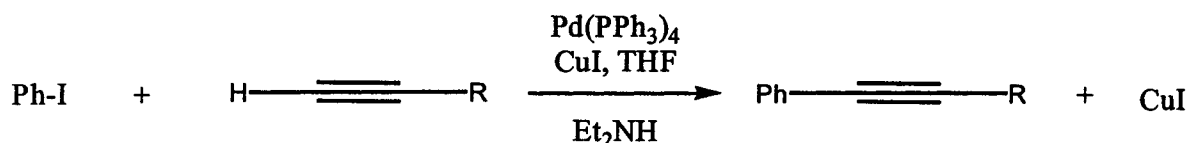
Scheme 5⁵³

2.1.3. Coupling by Thorand and Krause

In an attempt to optimize Sonogashira's coupling, variations in starting materials, and the order of addition of the alkyne and catalyst were made. It was observed that reactions completed in THF exhibited high yields, equal to or exceeding Sonogashira's yields after one hour (Scheme 6).⁵³ It was observed that the rate of reaction increased when THF was used as the solvent, while the rate of Glaser coupling decreased, when the alkyne was introduced with a slow, dropwise addition.^{53, 57} Additionally, various substituted aryl bromides and alkynes were used, and the

Sonogashira Pd(II) catalyst was replaced with a Pd (0) catalyst. A survey of the literature indicates that most enediyne syntheses are accomplished using modifications of Sonogashira's original procedure. The CuI co-catalyst is most commonly employed with Pd(PPh₃)₄, PdCl₂(PPh₃)₂, or Pd(OAc)₂(PPh₃)₂.^{45, 58,59,60}

Scheme 6⁵³

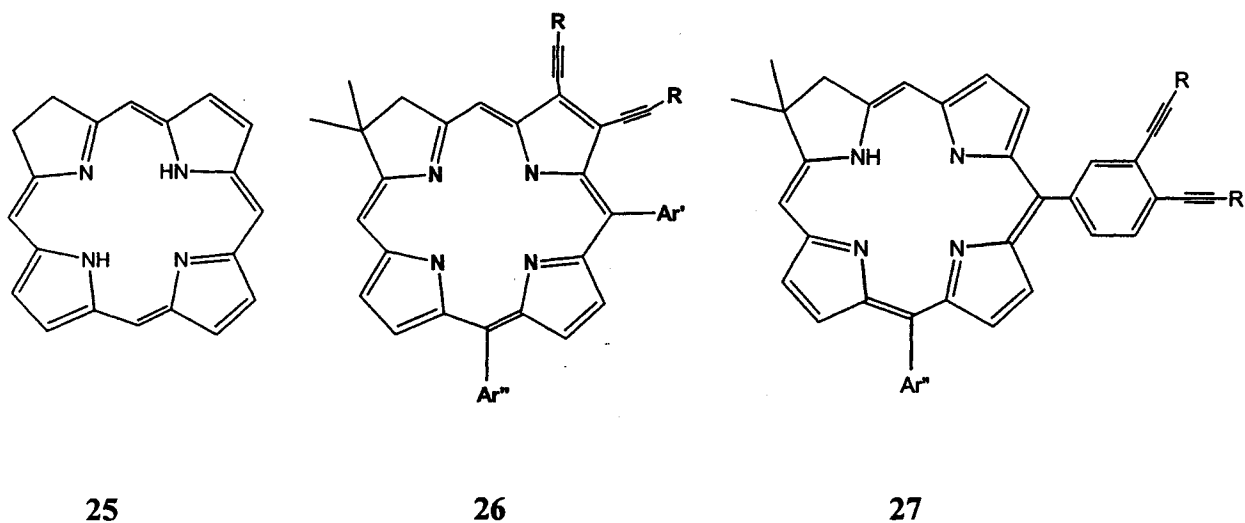


2.2. Synthesis of Nitrogenous Aromatic Enediynes

Recent literature has introduced some interesting potential nitrogenous aromatic enediynes. Kim and Russell synthesized and thermally cyclized a series of 1,2-diethynylheteroarenes (**8-10**).³² Their procedure utilized pressure reaction vessels, and due to these conditions, no Glaser coupling was observed. The kinetics of these species were studied and Arrhenius plots revealed the activation energies for subsequent cyclization at 165°C. Kim and Russell's studies, however, neglected thermal cyclizations, isolation and characterization of substituted alkynes, as all experiments were conducted on acetylenic enediynes. Additionally, no photochemical cyclizations were attempted.³²

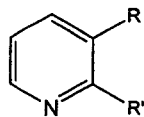
Another nitrogen containing aromatic that is of potential interest in enediyne syntheses is the pyrrole ring. Interest in this direction was piqued by the synthesis of chlorin (**25**).^{61, 62} The planar structure of chlorin could act as the delivery system desired in an enediyne analogue. It was envisioned that a 3,4-dialkynyl pyrrole, or a 3,4-dialkynyl benzaldehyde (**34**) could be utilized to

construct target enediyne chlorins **26** and **27**, respectively.

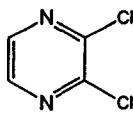


2.2.1 Synthetic Study of Nitrogenous Alkynyl Aromatics Using Sonogashira Coupling

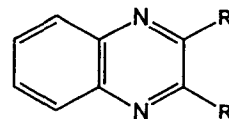
The focus of this chapter is the synthesis of starting materials for Sonogashira coupling reactions and the outcome of these coupling reactions. Readily available nitrogenous starting materials for coupling reactions were limited (**28-33**, **52**). The synthesis of sulfonyl esters (**35-40**, **53**) using trifluoromethanesulfonic anhydride or acid and methanesulfonyl chloride and the corresponding dihydroxy starting materials might yield compounds for coupling reactions. There are no available 3,4-substituted pyrrole compounds, therefore two different strategies were investigated (Scheme 7, pg 23).^{63, 64, 65, 66, 67} The resulting 3,4-disubstituted pyrrole would be subjected to coupling. Finally, the impact of varying the identity of the alkynes was investigated with respect to successful coupling. Four different commercially available alkynes were chosen to be used for this study, (**48-51**).



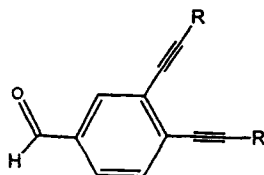
- 28** R, R' = OH
29 R = OH, R' = Br
30 R, R' = Cl
35 R, R' = OTf
36 R, R' = OMs
37 R = OMs, R' = Br
38 R = OTf, R' = Br
52 R = OH, R' = Cl
53 R = OTf, R' = Cl



31



- 32** R = OH
33 R = Cl
39 R = OTf
40 R = OMs



34



- 48** R = TMS
49 R = Ph
50 R = C(CH₃)₂OH
51 R = TIPS

Coupling reactions were performed using a published procedure in duplicate.³²

Tetrakis(triphenylphosphine)palladium(0) was the catalyst and cuprous iodide was the co-catalyst employed, with diisopropylamine as solvent. Diisopropylamine was chosen as the base, to match the conditions used in the literature procedure.³² Reactions were completed in 15 mL or 38 mL sealed tubes at temperatures determined by the literature reference.³²

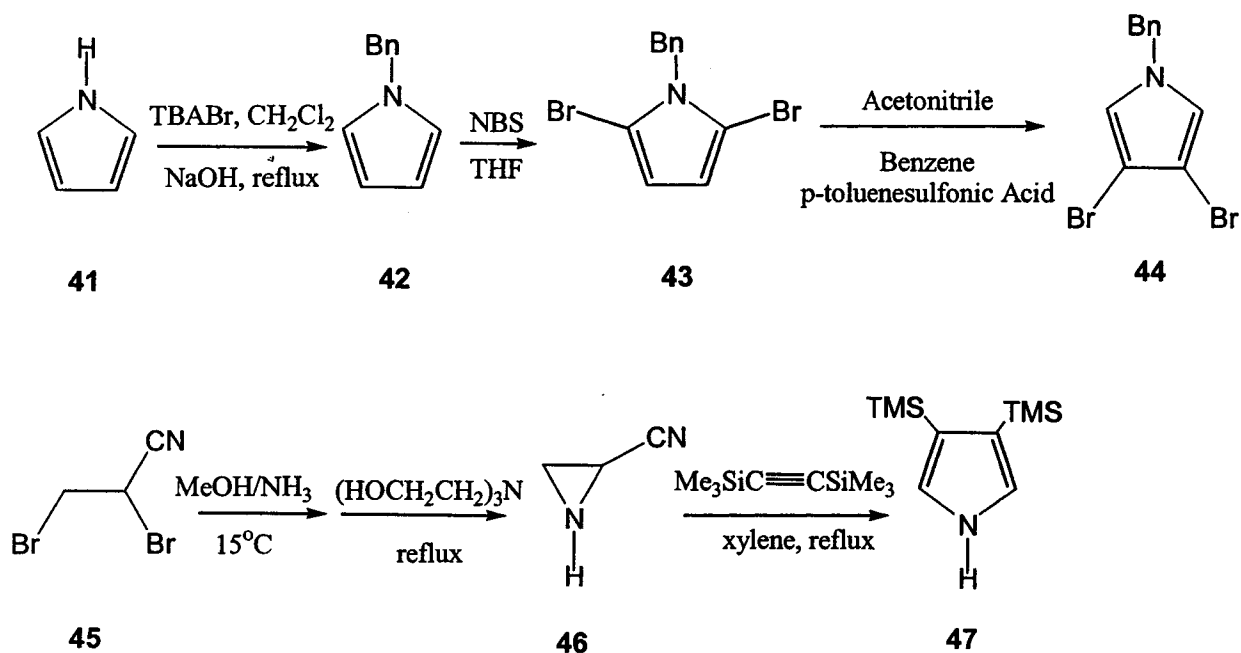
2.3 Results and Discussion - Nitrogenous Aromatic Eneidyne

The results of the synthetic study will be discussed in terms of percent yield trends in the following section. Prior to coupling, several starting materials had to be synthesized.

Compounds **28**, **29**, **32** and **52** were converted to their corresponding triflate and mesylate esters using the procedure discussed in Section 4.2.1 (See Experimental). Compounds **28**, **29** and **52**

were easily converted to their corresponding triflate and mesylate products in yields ranging from 58-99%. These products were carried forward into the coupling step. Compound **32** could not be converted to **39** or **40**, the only species recovered was starting material. As a result, this strategy was abandoned, resulting in compound **33** as the only quinoxaline starting material available for coupling.

Scheme 7^{63, 64, 65, 66, 67}



Two different approaches to the 3,4-dihalopyrrole were attempted (Scheme 7). The first conversion of pyrrole (**41**), to the 3,4-dibrominated product began with the addition of a protecting group to give **42**. This protected pyrrole was then brominated (**43**), and converted to the 3,4-dibrominated product, following procedures found in Section 4.2.1. The second approach

involved ring expansion of an aziridine, (**46**), using procedures listed in Section 4.2.1. These approaches were performed in accordance with published procedures, however, the results could not be reproduced consistently. The protection of **41** did not occur with reasonable yields despite repeated attempts. Additionally the isolated product **42** was found to be very unstable despite storage at -10°C under a nitrogen atmosphere. The subsequent bromination and conversion were never attempted. The synthesis of **46** was also attempted several times. The reaction did proceed and **46** was isolated in small amounts (5-10%), however it was found that **46** was very unstable even when frozen for short periods (1-2 days). Due to the instability of **46**, this approach was also abandoned.

2.3.1 Sonogashira Coupling Percent Yield Trends

Coupling to form compound **34** was attempted several times under various conditions. There is no published procedure for this reaction, therefore a procedure was created using the nitrogenous coupling procedure as a template.³² The first attempt involved coupling 3,4-dichlorobenzaldehyde at 80°C with TMS-acetylene. After 13 hours, GC and GC-MS spectra of the crude mixture were obtained and three peaks were observed. The largest peak by area corresponded to unreacted starting material, followed by a peak that corresponded to dimerized starting material. Finally, the smallest peak by area was found to be mono-coupled product. The amount of the product was quite small, and it could not be visualized on TLC. Therefore it was not isolated. In an attempt to increase the yield of the mono-coupled product or produce di-coupled product, the reaction temperature was increased to 100°C. A GC of the reaction mixture run after 13 hours showed only unreacted starting material and dimerized starting material.

To overcome the dimerization of the starting material, benzaldehyde was protected prior to coupling using ethylene glycol in aqueous acid. Several other coupling reactions had been completed by this point, and it was observed that the best yields had been obtained when coupling with alkyne **50**, so it was chosen for coupling with the protected benzaldehyde. When coupling was attempted at 80°C for 13 hours; three peaks were observed on the GC-MS. Two were identified as protected and deprotected benzaldehyde, while the third peak had a mass of 316 AU. The expected masses of mono- and di-coupled products were 250 and 314 AU respectively. The coupling was attempted at 100°C, however, only the protected and deprotected starting materials were observed. Due to the unreactive nature of this starting material, this approach was abandoned, and no further work towards the enediyne chlorin targets **26** and **27** was pursued.

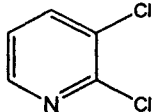
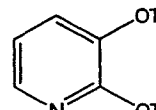
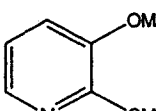
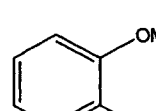
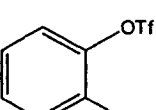
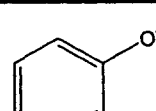
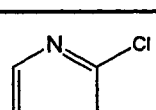
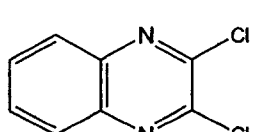
Initially, coupling was attempted between pyridine **38** and alkyne **51**. It was found that the mono-coupled compound was very unreactive, hence conditions were optimized so that coupling would proceed to give the di-coupled product. Mono- and di-coupled products were identified by GC-MS, however, all attempts to isolate the di-coupled product were unsuccessful. Despite flash chromatography and rotary chromatography the di-coupled products could not be separated from the starting material and mono-coupled products. It was due to this difficulty in separation that alkyne **51** was abandoned for the reactivity study.

The yields obtained for pyridine starting materials (Table 1) are remarkably different. Only compounds **38** and **53** produced the desired di-coupled pyridines. Compounds **35**, **36**, and **37** failed to couple and unreacted starting material was isolated, while compound **30** produced only mono-coupled products. The reactivity of compound **30** will be discussed in greater depth in relation to the quinoxaline and pyrazine starting materials. The poor reactivity of **35**, **36** and **37**

was puzzling as the leaving groups are generally thought to be better than the chlorides on compound **30** which did produce the mono-coupled compound. This may be a result of the stronger C-O bond of the triflate and mesylate groups compared to the weaker C-Cl bond. The mono-coupled product was not observed with quinoxaline starting materials, and only at lower temperatures for the pyrazine couplings. Procedures for the coupling reactions listed in Table 1 can be found in Chapter 4, Section 4.2.2.

Once the coupling reactions had been completed for compound **38**, it was discovered that the chloro-hydroxy starting material, **52**, was also commercially available. The hydroxyl group on the starting material was converted to the triflate **53** with a yield of 99%, utilizing identical conditions for the conversion of compound **29** to **38**. The coupling reactions were repeated using **53** in order to assess whether the established trend for halide substitution reactivity would be observed for nitrogenous starting materials. The coupling reactions with **48**, **50**, and **49** produced isolated yields of 63, 36 and 24 % of the di-coupled products, respectively. All the isolated yields were lower than the bromide starting material, **38**, as expected. The overall percent yield trend did not match that of compound **38**, however. It was expected that the highest isolated yield would be for the coupling reaction with alkyne **50**, based on the trends observed for the other starting materials. This may be a result of work-up and isolation procedures. Separation of the TMS-ethynyl di-coupled products and their respective starting materials was very difficult due to similar polarities for the mono- and di-coupled products. The isolated yields for these reactions may not reflect the actual conversion of the starting materials.

Table 1: Isolated Yields for Sonogashira Coupling Reactions

Compound	% Yield 48 ^a	% Yield 50	% Yield 49
	H—C≡C—TMS	H—C≡C—C(CH ₃) ₂ OH	H—C≡C—Ph
30 	0/49	0/0	0/0
35 	0/0	0/0	0/0
36 	0/0	0/0	0/0
37 	0/0	0/0	0/0
38 	74/trace	76/0	40/0
53 	63/trace	36/0	24/0
31 	74/trace	31/38 ^b , 76/0 ^c	52/0
33 	41/0	77/0	17/0

^a% di-coupled/% mono-coupled; ^b 80°C; ^c 100°C

The observed percent yield trends are easily rationalized using steric and electronic considerations. Dichlorinated starting materials **30**, **33**, and **31** were observed to show an overall reactivity increasing in that order. This was the expected result as previous studies have found that the 2- or 4-positions relative to the ring nitrogen, are reactive enough to di-couple even when the leaving group is chlorine.⁶⁸ A leaving group on the 3-position must be more reactive in a di-coupling reaction, eg. bromide, iodide or triflate ester. Compound **30** was observed to mono-couple only. This result may be a consequence of the 2- and 3-chloro leaving groups. From literature results, it was expected that coupling occurred at the 2-position which was supported by ¹H NMR spectroscopy. The spectrum of the product isolated from the reaction of compounds **30** and **48** showed one aromatic proton shifted up-field, with respect to the spectrum of the di-coupled product isolated from reactions of alkyne **48** with compound **38**. This indicated that the proton was adjacent to a chloro-substituted carbon.

Addition of a nitrogen in a 1,4- relationship to the pyridine nitrogen should result in greater coupling reactivity since both leaving groups would be in a 2-position to a ring nitrogen. This was the trend observed with pyrazine **31**, producing a higher coupling yield for alkynes **48** and **49**. Finally, it was expected based on previous work that the electronic nature of the second aromatic ring in quinoxaline **33** should reduce the leaving group ability of the chlorides.³² Generally, this was the trend observed for compounds **31** and **33**. The slightly higher yield for **33** with **50** may be a result of the isolation procedure or the non-optimization of the coupling procedure for **31** with **50**. The coupling reactions were not optimized once a reasonable, reproducible yield was obtained in duplicate, therefore the conditions used to react **31** and **50** may not have been optimized. The literature reference did not isolate the product of **33** with **48**, and

did not use compound **31**, therefore, our observed trends could not be compared.³² The most interesting observation is that although **33** produced a lower di-coupled yield than **31** when coupling with **48**, its corresponding mono-coupled product was more reactive than that of **31**. Trace amounts of mono-coupled **31** were observed by GC-MS, while no mono-coupled product arising from **33** was observed.

The general reactivity observed for the coupling reactions suggests that polarity of the mono-, di-coupled and the starting materials impacted the isolated yields. Alkyne **49** produced the least amount of isolated di-coupled products, although isolation was simple due to the high retention of the di-coupled products on silica. Reaction with alkyne **48** produced the di-coupled products in slightly higher isolated yields. The TMS di-coupled products were more difficult to isolate than their phenyl substituted counterparts. The similar polarities of the mono- and di-coupled products necessitated two purification steps, a long flash chromatography column followed by rotary chromatography. Despite following this procedure, not all of the di-coupled product could be separated from starting material. Finally, alkyne **50** produced the highest isolated yields. It is also possible that the electron withdrawing nature of this alkyne may have heightened the reactivity, or that the ability of a mono-coupled product to hydrogen bond with another equivalent of alkyne may have made the coupling of the second alkyne more energetically favourable. These products were easily separated from starting materials using flash chromatography. It was observed that the retention factor for di-coupled Ph and di-coupled tertiary alcohol enediynes were very different from those of their corresponding mono-coupled products, which simplified the purification procedures.

2.4 Reactivity Study of *meta*- and *para*-substituted iodobenzenes

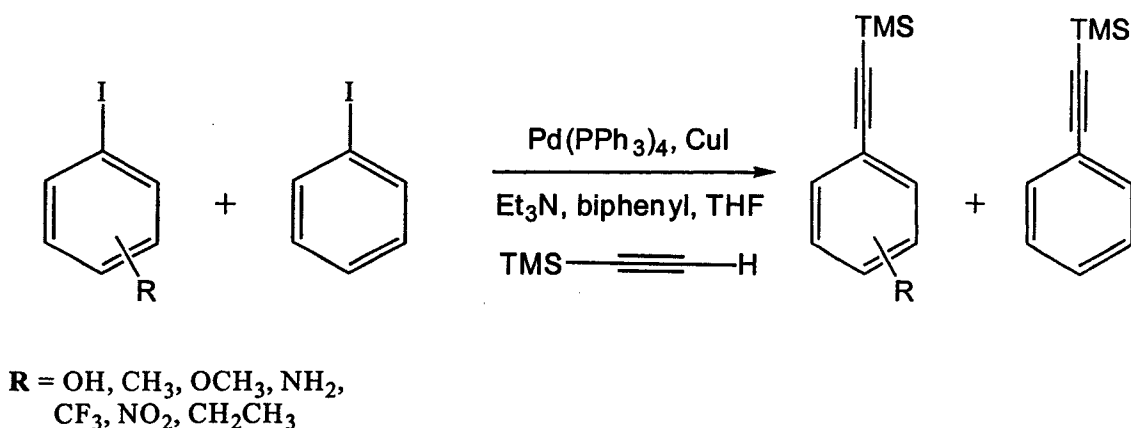
The resonance and inductive effects of a *meta*- or *para*-substituent on the coupling reaction were investigated by varying the EW and ED nature of the substituent. It has been established that EW groups in a position *para*- to a halide, will exhibit a dominant resonance and a smaller inductive effect, while EW groups in the *meta*- position to a halide exhibit inductive effects.⁶⁹ It has also been established that the reactivity in a coupling reaction increases with EW groups, and decreases with ED groups in the *para*- position.⁵⁵

2.4.1 Competition Reactions of *meta*- and *para*-substituted iodobenzenes

A series of substituted iodobenzenes were selected for this study. The available substituents ranged from strongly EW to ED. All *meta*- and *para*- isomers (except for 3-ethyliodobenzene) as well as the iodobenzene were commercially available. A *meta*- or *para*-substituted iodobenzene was placed in competition for an alkyne, with iodobenzene under palladium coupling conditions. In order to determine the relative reactivities, the decreasing amounts of starting materials were monitored using HPLC and an internal standard, biphenyl.

The reagents and amounts were chosen from literature references for Sonogashira coupling.⁵⁶ Tetrakis(triphenylphosphine)palladium (0) was chosen as the catalyst and cuprous iodide as the co-catalyst, as they have been found to provide efficient conditions. Triethylamine was chosen for the base, and TMS-acetylene as the alkyne. All reactions were performed at room temperature using 1 mmol of the *meta*- or *para*-substituted iodobenzene, iodobenzene, biphenyl and TMS-acetylene. Each reaction additionally contained 0.02 mmol Pd(PPh₃)₄, 0.04 mmol CuI, and 1.5 mmol Et₃N, (Section 4.2.5). The general reaction equation is shown in Scheme 8.

Scheme 8



Initially it was hoped that the *meta*- and *para*- isomers of iodobenzoic acid could be used as representatives of EW substituents. During the HPLC method development, it was observed that the amount of iodobenzoic acid decreased over short periods of time. This was attributed to ionization of the acid, which made it impossible to quantify. To compensate, both the methyl- and ethyl-esters of the iodobenzoic acids were prepared and isolated (55, 56, 57, 58).

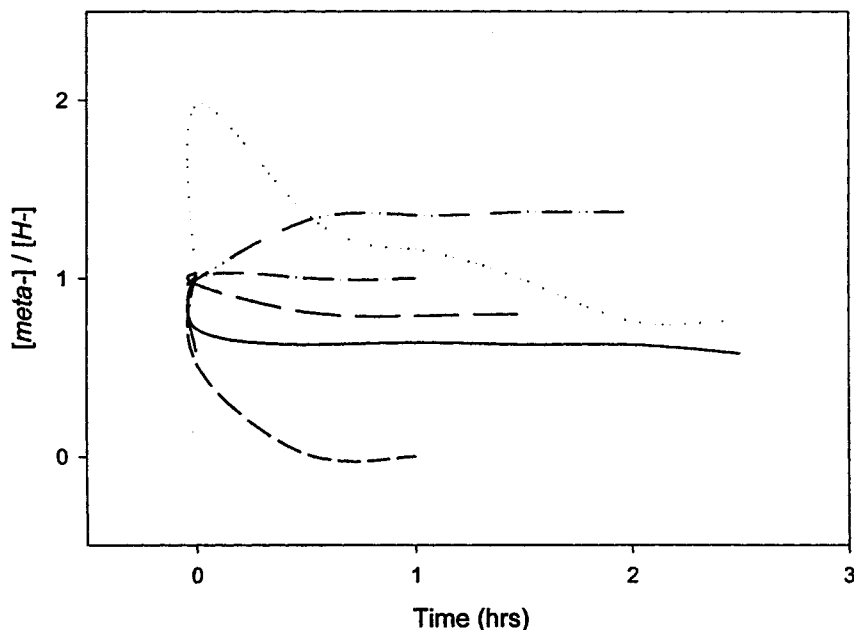
Unfortunately, a practical HPLC method could not be developed at this time which could separate these esters from iodobenzene and the biphenyl standard. As a result, the reactivity study had to proceed without these representatives.

2.4.2. Relative Reactivities for the Competitive Coupling Study

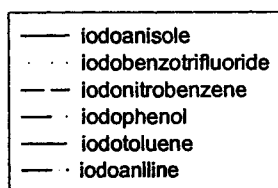
To establish the relative reactivities due to changing the electronic nature of the substituents, numerous competitive rate reactions were performed as described above, Section 4.2.6. Complete HPLC data can be found in Tables 12 to 18 in the Appendix. Concentration ratio versus time graphs were constructed to analyse the data.⁷⁰ Data was plotted until no further

reaction occurred, either until all starting material had reacted, or until the isomer/iodobenzene ratio did not change over three time points. Graph 1 shows the relative reactivity between *meta*-substituted iodobenzenes and iodobenzene, while Graph 2 shows the relative reactivity observed for *para*-substituted iodobenzene and iodobenzene. Initial samples were analysed prior to catalyst and TMS-acetylene addition to calculate response factors, Section 4.2.4. Time zero samples were extracted at the time of TMS-acetylene addition, and reaction times reported were relative to this time point

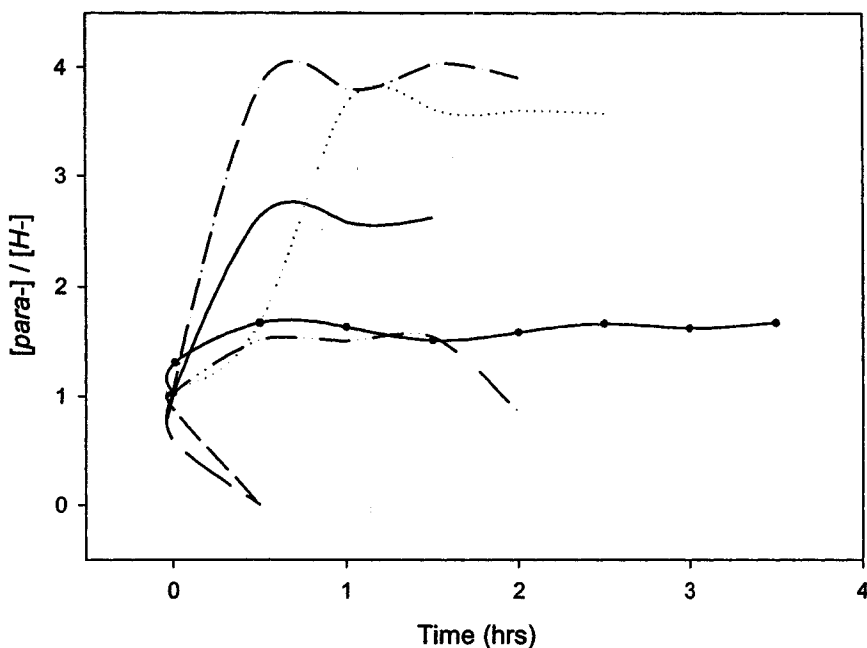
Graph 1
Relative Reactivity *meta*- vs *H*-substituted Aryl Iodides



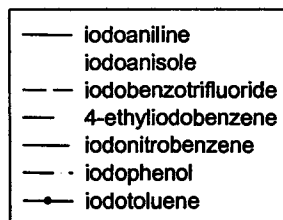
*Note: The decrease in starting material concentration was monitored.



Graph 2
Relative Reactivity *para*- vs *H*-substituted Aryl Iodides



*Note: The decrease in starting material concentration was monitored.



The kinetics of these reactions are not known. The experiments were designed in an effort to establish relative reactivity trends by measuring the disappearance of the starting materials with respect to an internal standard. Similar competitive rate reactions have previously been completed in our group, in which the products were isolated and it was observed that disappearance of the starting materials corresponded to the appearance of products.⁷⁰ Based on σ_m values, the relative

reactivities were expected to increase in the order: $\text{NH}_2 < \text{CH}_3 < \text{H} < \text{OCH}_3 < \text{OH} < \text{CF}_3 < \text{NO}_2$.⁷¹ The reactions were set up as in Section 4.2.2 and monitored by HPLC every half hour. From analysis of the curve for the *meta*-phenol it was obvious that iodobenzene was more reactive than *meta*-iodophenol, (Table 2, pg 35, Entry 4, R=*m*-OH). This result was unexpected due to the inductively withdrawing nature of the hydroxy substituent in the *meta*-position. This result also indicated that although the hydroxy substituent is EW in the *meta*- position, it does not affect the ring in such a way as to make it more reactive than iodobenzene. It was speculated that the acidity of the hydroxyl proton affects reactivity, possibly through interference with the catalyst or base. Unexpected reactivity was observed for the reaction of *meta*-iodotoluene, Entry 2. The ED nature of the methyl substituent should have made the compound less reactive than iodobenzene, however, the opposite effect was observed. This indicated that the weakly donating nature of the methyl- substituent was not very different from iodobenzene, and with similar reactivities, iodobenzene slightly less reactive than iodotoluene. The *meta*-iodoaniline (Entry 1) also showed interesting and unexpected reactivity. Although NH_2 is inductively EW, and initially was more reactive than iodobenzene, its reactivity decreased to equal that of iodobenzene. This may be a result of the decreased concentration of iodoaniline that resulted in less competitive conditions or that, in this case, the weak inductively withdrawing properties of the aniline do not alter the reactivity an appreciable amount. Reaction of *m*-iodo- α,α,α -trifluorotoluene (Entry 5) also shows interesting reactivity. The EW *m*-iodo- α,α,α -trifluorotoluene initially showed a lower reactivity than iodobenzene. The reactivity then increased to greater than the iodobenzene, which was the reactivity that was expected. This initial poor reactivity is very puzzling. The CF_3 substituent must affect the electronic nature in a deactivating manner, until the concentration of

iodobenzene decreased to a level where the reaction with iodo- α,α,α -trifluorotoluene became more competitive.

Table 2: Concentration Ratios for Competitive Rate Reactions Between *meta*- and H-substituted Aryl Iodides

Time (hrs)	Entry 1 R = NH ₂	Entry 2 R = CH ₃	Entry 3 R = OCH ₃	Entry 4 R = OH	Entry 5 R = CF ₃	Entry 6 R = NO ₂
σ_m^{71}	-0.16	-0.069	0.115	0.121	0.43	0.71
	[<i>m</i>]/[H]	[<i>m</i>]/[H]	[<i>m</i>]/[H]	[<i>m</i>]/[H]	[<i>m</i>]/[H]	[<i>m</i>]/[H]
initial	1.02	1.03	1.03	1.01	0.99	1.02
0.0 TMS addition	0.59	0.96	0.71	1	1.98	0.5
0.5	1	0.81	0.63	1.32	1.36	0.01
1	1	0.79	0.64	1.35	1.16	0
1.5	1	0.8	0.63	1.37	0.99	
2			0.63	1.37	0.76	
2.5			0.58		0.77	

Entry 3, the *meta*-iodoanisole, also reacted faster than iodobenzene from the time zero measurement until the reaction was stopped. This reactivity was attributed to the inductively EW nature of the substituent. Comparison of the iodophenol, Entry 4, and the iodoanisole, Entry 3, is interesting. The methoxy substituent in *m*-iodoanisole is also an EW group, and showed a greater reactivity than iodobenzene as expected. It is interesting that two related EW compounds, Entries 4 and 3, show such differing reactivity. Finally, the strongly EW NO₂ group in *meta*-

iodonitrobenzene, Entry 6, shows considerably high reactivity. The nitrobenzene starting material had completely reacted within 1 hour. In this case, the strongly EW nature of the nitro-substituent affects the reactivity of the ring greatly, even though it can only affect it inductively. Overall, the results show that inductive effects do not influence reactivity, especially when the substituents are not strongly EW or ED. When the substituents are strongly EW, as in the case of Entry 6, the nature of the ring is affected and the reactivity increases greatly. Similar to the expected relative reactivities stated above, the reactivity trend was found to be: $\text{OH} \ll \text{NH}_2 < \text{H} < \text{CH}_3 < \text{CF}_3 < \text{OCH}_3 < \text{NO}_2$. This differed somewhat from the expected reactivity trend, Table 2. This was attributed to the possible interactions between the iodophenol and other reagents as discussed above, shifting its reactivity relative to the other substituents examined. The order of iodobenzene and iodotoluene were also switched relative to the expected trend. This can be explained by the σ_m values for iodobenzene and iodotoluene being close in value (0.00 and 0.069 respectively).

Based on σ_p values, the reactivity for the *p*-substituted iodobenzenes was expected to follow the trend: $\text{NH}_2 < \text{OH} < \text{OCH}_3 < \text{CH}_3 < \text{CH}_2\text{CH}_3 < \text{H} < \text{CF}_3 < \text{NO}_2$.⁷¹ The relative reactivities for this series of the substituents are presented in Table 3. *p*-iodonitrobenzene and *p*-iodo- α,α,α -trifluorotoluene, Entries 6 and 7 reacted very quickly, with none of the starting materials left after the first half hour of the reaction in both reactions. Iodonitrobenzene showed a greater reactivity than *p*-iodo- α,α,α -trifluorotoluene, which was expected as it has the largest σ_p value of the two compounds. The high reactivity of both compounds can be attributed to strong EW nature of their substituents in a resonant position and their large positive σ_p values.

Table 3: Concentration Ratios for Competitive Rate Reactions Between *para*- and H-substituted Aryl Iodides

Time (hrs)	Entry 1 R = NH ₂	Entry 2 R = OH	Entry 3 R = OCH ₃	Entry 4 R = CH ₃	Entry 5 R=CH ₂ CH ₃	Entry 6 R = CF ₃	Entry 7 R = NO ₂
σ_p^{71}	-0.66	-0.37	-0.268	-0.17	-0.151	0.54	0.778
	[p]/[H]	[p]/[H]	[p]/[H]	[p]/[H]	[p]/[H]	[p]/[H]	[p]/[H]
initial	1.01	1.01	1.02	1.03	1.05	1.04	1.03
0	1.07	1.14	1.09	1.31	1.05	0.86	0.57
0.5	2.63	3.82	1.67	1.67	1.51	0	0
1	2.58	3.8	3.66	1.63	1.5		
1.5	2.62	4.03	3.61	1.51	1.54		
2		3.9	3.6	1.58			
2.5			3.57	1.66			
3				1.62			
3.5				1.67			

Conversely, the ED substituted compounds, Entries 1-5, exhibited the reverse reactivity. Iodophenol, Entry 2, was observed to have the lowest reactivity. Iodoanisole, Entry 3, was observed to have a slightly greater reactivity, although it was still less reactive than iodobenzene. This reactivity can be attributed to the lower ED nature of the OCH₃ substituent compared to the OH substituent. A large jump in relative reactivity was observed with the reaction of iodoaniline, Entry 1. Although less reactive than iodobenzene, iodoaniline was more reactive than iodophenol and iodoanisole. This reactivity trend was unexpected as the NH₂ substituent is more ED than

both OH and OCH₃ substituents. It was postulated that for this particular mechanism, the two lone pairs of electrons on the oxygen atoms in the OH and OCH₃ substituents must increase the π -donation into the ring compared to aniline. The alkyl substituted iodobenzenes were slightly more reactive, due to their weaker ED nature. *p*-iodotoluene, Entry 4, was quickly out-competed by iodobenzene and the reaction rate levelled off by the end of first half hour of the reaction. *p*-Ethyliodobenzene, Entry 5, also was out-competed by iodobenzene within the first half hour of the reaction. The calculated $[p]/[H]$ ratio was larger for *p*-iodotoluene than the *p*-ethyliodobenzene. This indicated that *p*-ethyliodobenzene was more reactive than *p*-iodotoluene.

The observed trend of reactivity was: OH < OCH₃ < NH₂ < CH₃ < CH₂CH₃ < H < CF₃ < NO₂. The observed trend is similar to that expected for the *para*-substituents based on the σ_p , except in the location of the *p*-iodoaniline. It was predicted to have a higher reactivity than that of *p*-iodoanisole and *p*-iodophenol. This discrepancy may be due in part to interference of the starting materials with the catalyst, or the base used, and further analysis is required to determine the cause of this reactivity. Analysis of Graphs 1 and 2 led to the conclusion that overall reactivity is governed by the ED and EW character of the substituents, as predicted.⁵⁵ The overall trends, however, were somewhat difficult to explain. The reactivity trends for *m*-substituted iodobenzenes indicated that inductive effects do not affect the reactivity to a large degree. In contrast, the reactions of *p*-substituted iodobenzenes showed remarkable reactivities. Influence of the EW and ED nature of the substituents was observed to drastically affect the reactivity of the compounds towards coupling.

2.4.3. Conclusion

In summary, several conclusions may be drawn. It is apparent from examination of the percent trends for Sonogashira coupling of nitrogenous heterocycles that the role of sterics is crucial to reactivity. The steric demands of the leaving group on the heterocycle affect the reactivity of the system, as do the steric demands of the alkyne. The best isolated yields were obtained when an excess of 3-methyl-2-butyne-3-ol, **50**, was employed as the alkyne for coupling. This was likely a result of the relative affinities for silica for the starting materials, di-coupled and mono-coupled products. Additionally, the identity of the leaving group was found to impact the overall reactivity. For the pyridine starting materials, for which a number of substituted compounds were available, the nature of the bond was found to dictate the coupling reactivity. Leaving groups such as di-substituted triflic and mesylate leaving groups were unsuccessful in coupling, while smaller chlorine leaving groups were more reactive and mono-coupled. This was a surprising result, as mono-triflates have been successful in coupling reactions. This poor reactivity may be a result of steric inhibition for complex formation when coupling a di-sulfonyl ester. A combination of two good leaving groups, bromide and triflate, produced the compound most reactive to coupling, **38**. These coupling trends were attributed to the strength of the bond between the C and the leaving group. The electronics of the ring, through the addition of nitrogens, as well as extension of the ring system, noticeably affected the reactivity towards coupling. In accordance with results already published, the addition of nitrogens to the heterocycle improve reactivity, while addition of electron donating aryl rings do not.^{32, 67}

The effect of resonance and inductive forces on the reactivity of a compound toward Sonogashira coupling was also discussed in this chapter. The comprehensive relative reactivity

study correlated with previously established data and hypotheses.⁵⁵ It was observed that substituents that were in a *para*-position to an aryl halide exerted a large resonance and mesomeric effect that governed the reactivity. The overall reactivity trend was very similar to the σ_p and σ_m values for the substituents. The trends for the effects of substituents in the *meta*-position were not always so obvious. Strongly EW substituents still increased reactivity through induction. ED substituents, are expected to decrease the reactivity. The weaker ED substituent -CH₃ actually caused a slight increase in reactivity, which was surprising. Comparison of both the *meta*- and *para*- results indicated that the larger effect occurred when the substituent was in a resonant position to the aryl halide. A less pronounced effect occurred when the substituent was not in a resonant position, where weaker inductive forces played a role.

This chapter has focussed on the formation of enediyne analogues and the reactivity of their precursors towards coupling reactions. The next chapter focusses on the ability of these analogues to undergo thermally and photochemically induced Bergman cyclizations. A reactivity study of these analogues, with regards to their electronic and steric natures will be presented, as well as a assessment of their potential for use in anti-cancer trials.

CHAPTER THREE

A SYNTHETIC STUDY INVOLVING THE BERGMAN CYCLIZATION

3.1 Introduction

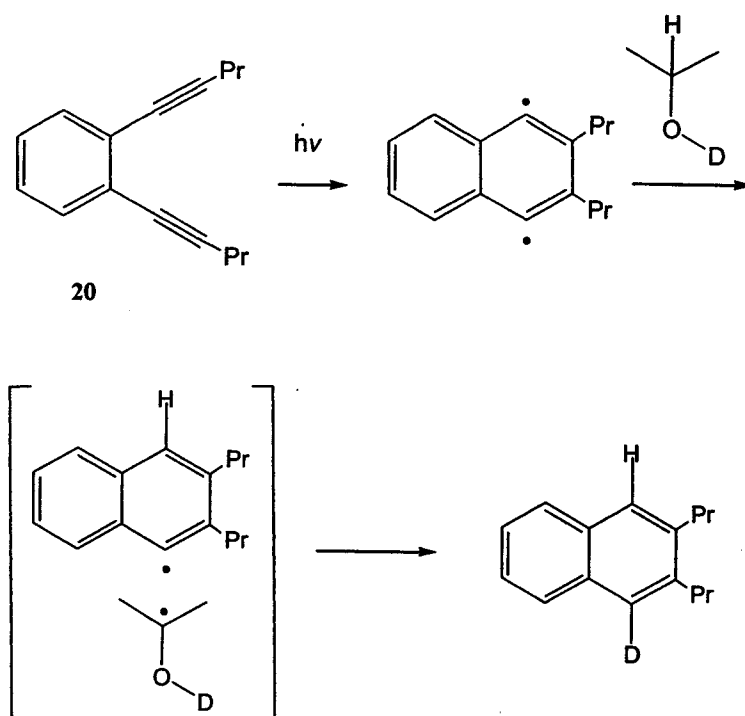
The success of a potential enediyne analogue drug relies on a reproducible and selective trigger for the Bergman cyclization which leads to cell death. The requirements for a successful enediyne analogue were discussed in detail in Chapter One, and the use of the Sonogashira coupling reaction as a route to form these compounds was discussed in Chapter Two. This chapter will focus on both the photochemically and the thermally induced cyclization reactions. An inspection of recent literature indicates that a great deal of study has concerned thermal cyclizations, while photochemical cyclizations have been largely ignored. This study was designed to add to the body of knowledge for both thermal and photochemical triggering of nitrogenous aromatic enediynes.

3.1.1 Thermal Bergman Cyclization

As cyclizations were discussed in Chapter One, only a brief summary will be given in this section. The majority of the literature concerning thermally induced Bergman cyclizations has suggested that the contributing factor in successful cyclization is acetylenic substitution. Work by Grissom *et al.* compared Bergman's estimated energy of activation for an acyclic enediyne with that of an acyclic aromatic enediyne.³⁶ They found that these values did not differ greatly, and thus proposed that the major effect on energy of activation is a result of the added substituents on the acetylenic groups of their study compounds. Adding support to this theory

was a study completed on acyclic analogues (14, 16 and 17).³⁷ Most interesting to our group was the evidence of intramolecular bonding in compound 17 that dramatically reduced its cyclization temperature. It was postulated that this may occur in compounds with an alkynyl substituent containing a hydroxy group. This was observed in the preparation of decoupled tertiary alcohol products as discussed in Chapter Two. I questioned whether this would affect the reactivity to cyclization and be observed in an increased yield or rate of reaction for the cyclization reactions.

Scheme 9¹⁴



3.1.2 Photochemical Bergman Cyclization

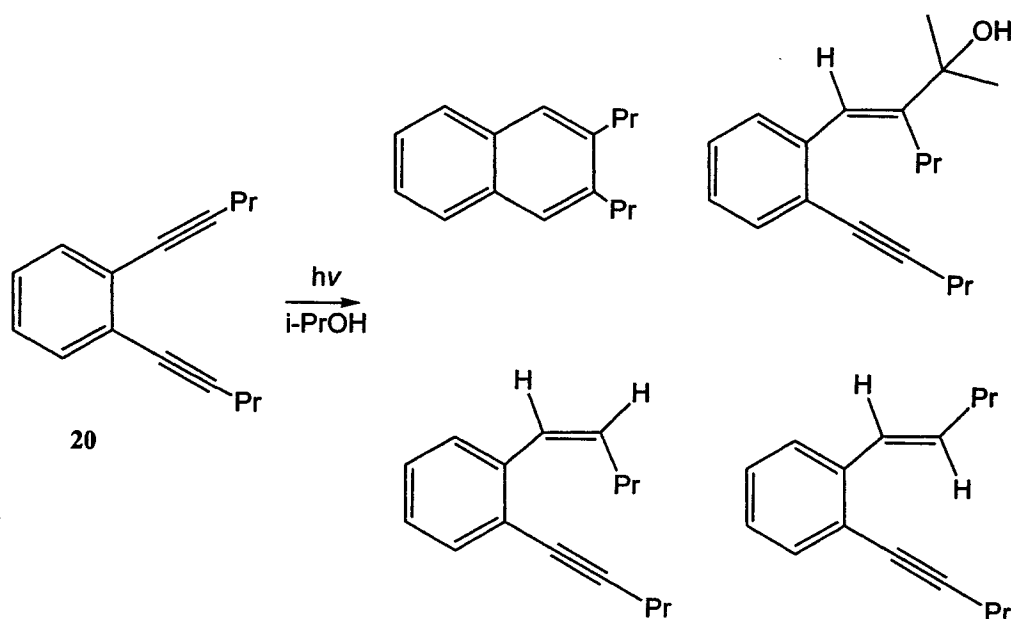
Photochemical Bergman rearrangement was first reported in 1994 by Turro and Evenzahav.¹⁴ The products isolated were consistent with the formation of a radical pair that was generated by hydrogen abstraction from the protic solvent followed by the disproportionation of the radical solvent species (Scheme 9). Thermal cyclizations completed in carbon tetrachloride result in formation of a cyclized dichloro compound;³² this cyclized dichloro compound should be the product of the photochemically induced cyclizations using carbon tetrachloride as the solvent if this is the mechanism of the reaction. More recent work by Turro and Evenzahav has suggested that the success of photochemical cyclizations depends greatly on the identity of the acetylenic substituents.¹¹ More specifically, compounds that are more rigid have a higher probability of cyclizing. This was evident from the photocyclization of two enediynes **20** and **21**. Enediyne **20** did successfully cyclize, however photo reduced products were also isolated (Scheme 10). It is believed that these side products arise when the excited biradical relaxes to a triplet state through intersystem crossing. In contrast, enediyne **21**, when irradiated, produced only the cyclized product. This is believed to occur because the phenyl rings force the acetylenic carbons into a more rigid conformation than the propyl substituents. This rigidity lowers the probability of other relaxation processes. Interestingly, energy minimization calculations for the excited state revealed that the *cd* for compound **20** to be between 4.078 and 4.120 Å. The same calculation for compound **21** yielded a *cd* of 3.926 Å. Both of these distances are much larger than the 3.31 Å *cd* that has been proposed to be stable at 25°C, according to Nicolaou's hypothesis.²⁴

3.2 Cyclizations of Nitrogenous Aromatic Eneidyne

The work of Kim and Russell did not address several issues.³² Firstly, a comprehensive study of the reactivity of several nitrogenous starting materials and alkynyl substituents was not completed. This issue was addressed in Chapter Two. Additionally, the effect of acetylenic substituents on the reactivity toward the Bergman cyclization was not researched.

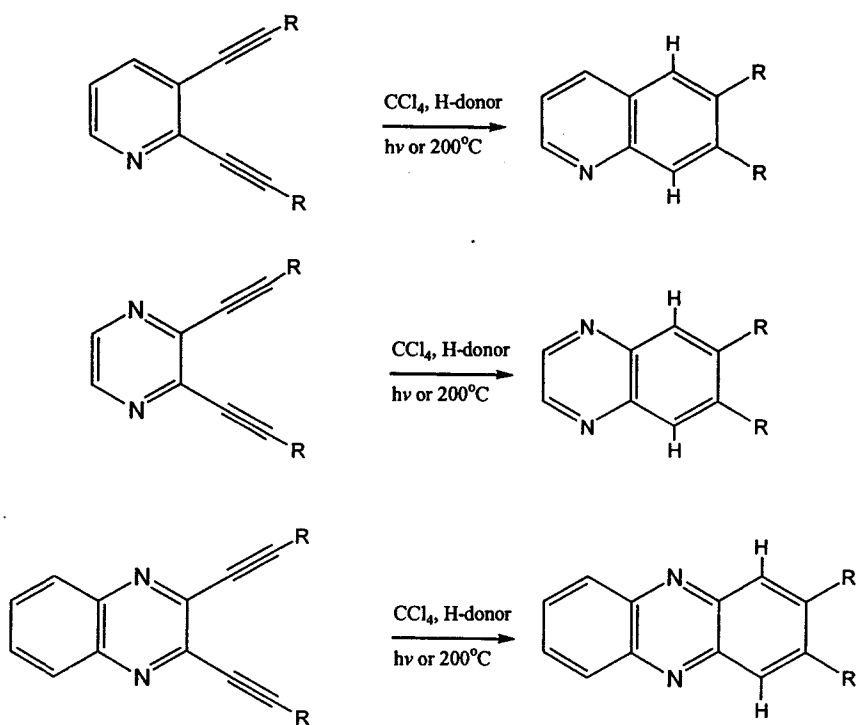
Photochemistry of nitrogenous enediynes was not attempted. Finally, the effect of a fused aromatic ring was not studied through the comparison of quinoxaline and pyrazine starting materials.

Scheme 10¹¹



3.3 Results and Discussion

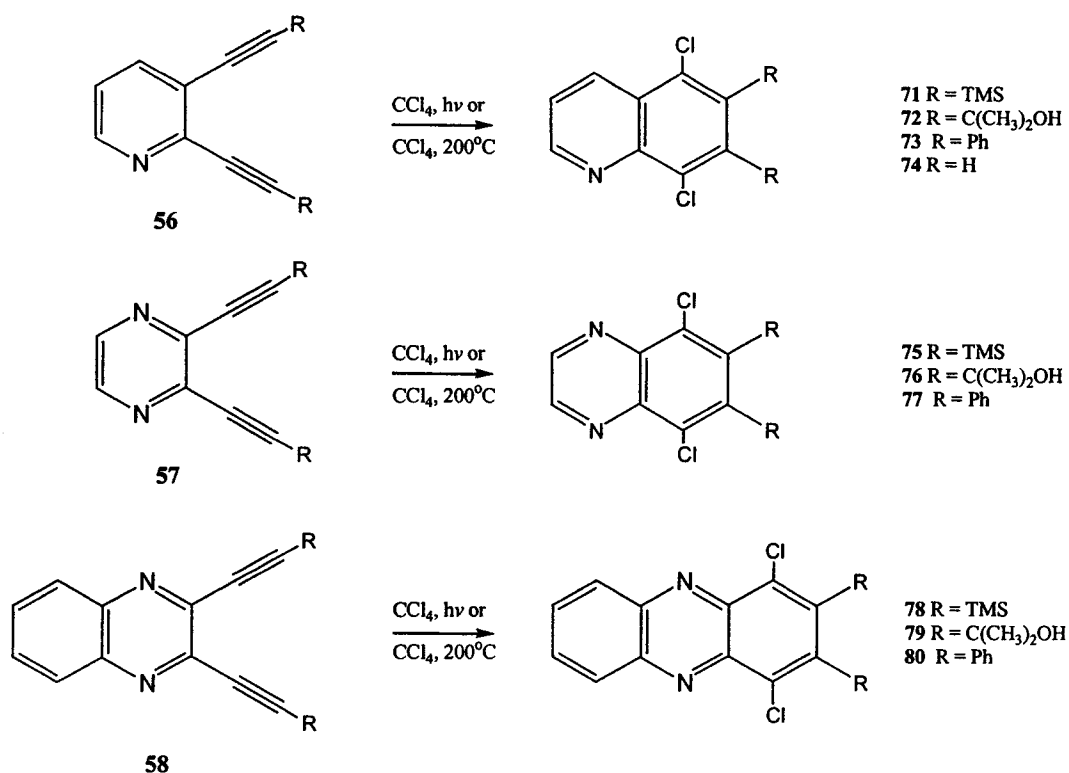
Scheme 11



The initial objective of this study was to thermally and photochemically cyclize the enediyne analogues in the presence of an hydrogen donor (Scheme 11). These reactions were completed, however, difficulty arose during the identification of the products. GC-MS eventually revealed that the enediyne starting material and the cyclized products coeluted on the GC and GC-MS, and could not be resolved. This made identification and isolation of the products virtually impossible. It was concluded that alternative cyclization conditions would have to be employed. Kim and Russell had successfully thermally cyclized enediynes in carbon tetrachloride, and isolated the dichloride products. According to Turro and Evenzahav, it was

proposed that irradiation in carbon tetrachloride should yield cyclized products in the same manner as irradiation in other solvents.¹⁴ All cyclizations were completed in carbon tetrachloride and the dichlorinated products were characterized by GCMS and ¹³C NMR spectroscopy (Scheme 12). More specifically, photochemical cyclizations were monitored hourly by GC to determine optimum reaction times, while thermal cyclizations were reacted for twelve hours, and then evaluated by GC. Initially, thermal reactions were performed at 165°C, as in the literature reference.³² This temperature produced no reaction after 48 hours, which is a typical half-life time for the unhindered enediynes.³² To compensate for the steric interactions of the acetylenic substituents, the reaction temperature was increased to 200°C, however, this temperature also failed to produce the desired cyclized products.

Scheme 12



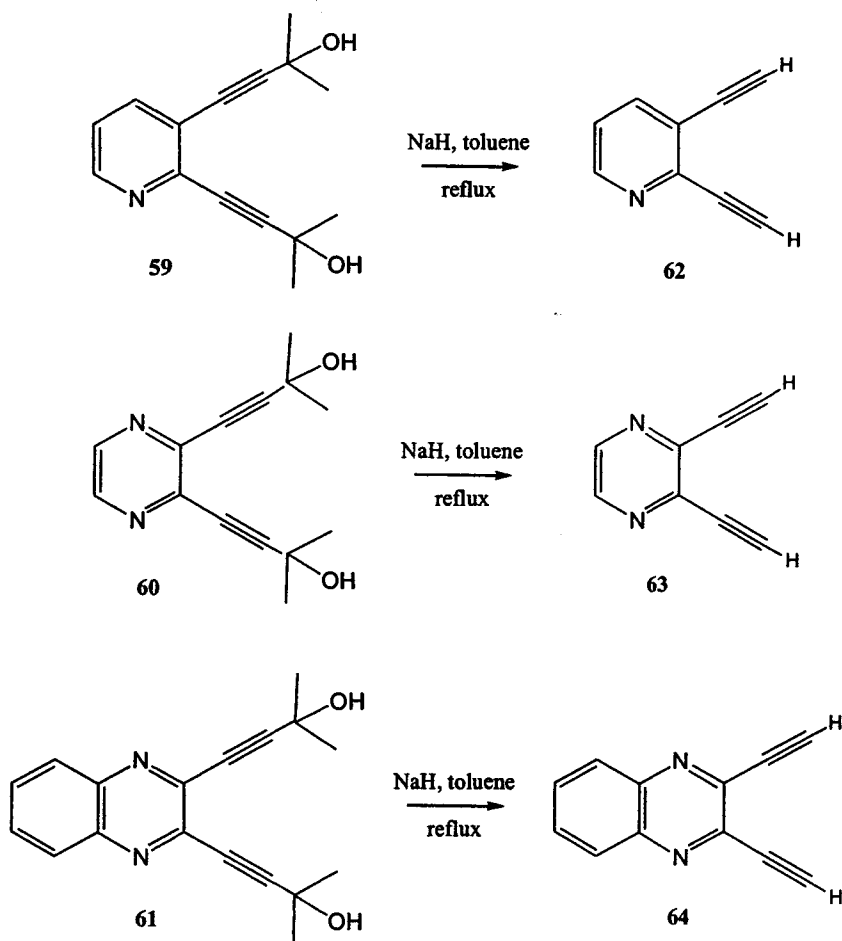
Initially, photochemical cyclizations were carried out in a quartz tube protected with a Pyrex shield. This procedure was modified to determine the effect of the shield on the reactivity, entries 1 and 11 Table Four, pg 50. Polymerization was found to be a major side reaction. It was determined that in addition to calculation of the cyclization yield, that the disappearance of starting material should also be calculated. This was accomplished through calculation of the conversion yield, Section 4.2.4. The overall cyclization yield remained unaffected by the presence or absence of the shield, however, the conversion yield and the major product observed from polymerization was greatly increased in the absence of the shield.

Photochemical products observed via GC and GC-MS were not easily isolated, due to the low yields and similar polarity to their respective starting materials. Many attempts at chromatography failed to isolate the cyclized products observed by GC-MS. As an alternative, the response factor for the enediyne starting materials were calculated using a standard method.⁷²
⁷³ Since the chemical formulae of the enediynes and cyclized products differed only by two chlorine atoms, the response factors could be used to calculate the molarity of the product using an internal standard. The crude mixture was run on GC with biphenyl as the internal standard and cyclized and conversion yields were calculated.^{72,73}

Once the photochemical and thermal reactions had been completed, and the GC yield determined, NMR spectroscopic data was acquired for the crude mixture. Unfortunately, due to the high starting material to product ratio, the product peaks were masked by the starting material peaks. This made assignment of the product peaks difficult. Additionally, due to the high concentration of the starting material, concentration effects and peak shifting were observed, therefore the starting material peaks could not simply be subtracted from the spectrum. To

compensate for this, the crude mixtures were subjected to rotary chromatography preceding NMR spectroscopy in an effort to remove some of the interfering materials. This process was very successful and ^{13}C NMR spectra were obtained for the suspected cyclized products.

Scheme 13



In order to complete the areas studied by Kim and Russell, the photoreactivity of the unhindered enediynes required further analysis. To synthesize these enediynes, one of the previously isolated enediynes would have to be deprotected. Literature procedures were

available for the deprotection of TMS-ethynyl³² and 3-hydroxy-3-methylbutynyl substituents.⁷⁴

The 3-hydroxy-3-methylbutynyl starting materials were chosen since the polarity of the unhindered enediyne would be different than the starting material and would allow easy separation (Scheme 13).

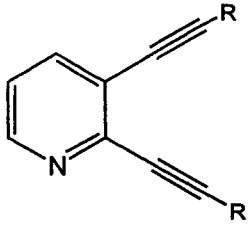
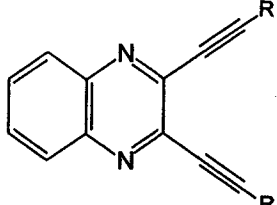
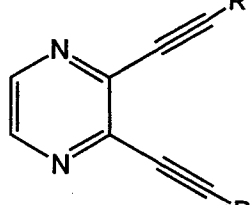
The deprotections were completed, and isolations completed without trouble. The yields for the deprotections of **60** and **61** were poor, at 7 and 4%, respectively. Enediyne **59** deprotected well with a 52% yield. These poor yields were not due to poor conversion of the starting materials, as little starting material was observed on the GC. During the work-up, a large quantity of dark, insoluble material was observed which suggested that the low yields were due to polymerization or degradation of the starting materials due to the reaction conditions. It was concluded that, due to the poor yields and availability of the enediynes, photochemistry and thermal reactions would not be completed for compounds **63** and **64**. Irradiation experiments were limited to **62** since it was available in larger amounts.

3.3.1 Percent Yield Trends

The yields for thermal and photochemical cyclization reactions are presented in Table 4. According to the literature reference, the deprotected analogues (**62** and **64**) successfully cyclize at 165°C (Table 4, Entries 5 and 9).³² The thermal cyclizations did not proceed at 165 or 200°C for the related hindered enediynes synthesized in Chapter Two, compounds **59-61** and **65-70**. The crude mixtures were tested by GC and found to contain only unreacted starting material with little evidence of polymerization. It was concluded that this was largely a steric effect, and that the reaction energy was not high enough to overcome the energy of activation for thermal cyclization.

Reactions at higher temperatures were not attempted, due to the limitations of the heating bath and the stability of the sealed reaction vessels.

Table 4 - GC yields for cyclization reactions

Enediyne	Entry	R	Thermal	Photochemical cyclized/converted
	1	TMS ^a (65)	-	<1/79
	2	TMS ^b (65)	0	1/20
	3	C(CH ₃) ₂ OH ^b (59)	0	0
	4	Ph ^b (66)	0	4/16
	5	H (62) ^b	trace ³²	0
	6	TMS ^b (67)	0	2/19
	7	C(CH ₃) ₂ OH ^b (61)	0	0
	8	Ph ^b (68)	-	0/66
	9	H (64)	81 ³²	-
	10	TMS ^b (69)	0	3/28
	11	C(CH ₃) ₂ OH ^b (60)	0	0
	12	Ph ^b (70)	0	<1%/1
	13	Ph ^a (70)	-	4/100
	14	H (63)	-	-

^aWithout Pyrex shield, ^bWith Pyrex shield

The photochemical cyclizations exhibited very different trends from the thermal reactions.

The crude mixtures were also subjected to GC and found to have high conversion rates. GC-MS indicated that much of the starting materials had been polymerized. The 3-hydroxy-3-methyl-substituted enediynes failed to react at all. It was postulated in the previous chapter that internal hydrogen bonding may occur within the substituent, which would account for the higher yields in the coupling reactions. It was evident from the results of the cyclization studies that internal hydrogen bonding either does not occur, or is not an important factor in the reactivity of the 3-hydroxy-3-methyl-substituted enediynes. Additionally, very little of the 3-hydroxy-3-methyl-substituted enediynes dissolved in the carbon tetrachloride solvent, which may also have been a large factor in the poor reactivity.

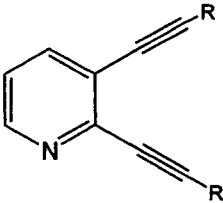
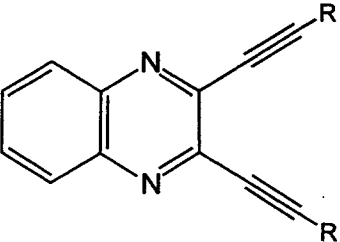
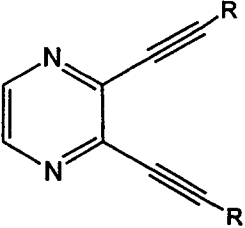
The TMS enediynes **65**, **67**, and **69**, produced their corresponding cyclized products after five hours of irradiation (**71**, **75**, **78**). Compound **65** cyclized with a 1 % yield, while compound **69** cyclized with a 3% yield. This is an interesting trend, because these results mimic the relative reactivities observed for the coupling reactions. This suggested that added nitrogens in the ring increase the reactivity toward photochemical cyclizations. Compound **67** cyclized with a 2 % yield. This also follows the results of the coupling reactions. The added aromatic ring was found to decrease the reactivity toward coupling reaction for coupling with TMS-acetylene (**48**) and phenyl-acetylene (**49**). The Ph enediynes **66** and **70** produced their corresponding cyclized products (**73** and **80**). The cyclizations for the phenyl-substituted enediynes (**66**, **70**) did not follow the trend discussed above. Enediyne **66** and enediyne **70** both cyclized with a 4 % yield. It was expected that yield for the cyclization of enediyne **70** would be slightly higher due to the added nitrogen. It was clear that the presence of the activating phenyl rings was a more important factor than the activation gained by the added nitrogen.

The cyclizations of enediynes **67** and **68** were interesting. It was expected that the cyclization yields for these compounds should lie below the yields observed for the pyrazine enediyne derivatives. This was observed for the TMS-substituted enediynes, with a 2 % cyclization yield for enediyne **67**. This was the result expected based on the reactivity trend observed for the coupling reactions. The added aromatic ring in the quinoxaline was found to deactivate the compound towards coupling, which produced lower yields than for the pyrazine derivatives. This trend was also observed for the cyclization of enediyne **68** compared to the cyclization of enediyne **70**. It was expected that the deactivating nature of the quinoxaline backbone would produce a lower cyclization yield for enediyne **68** than for enediyne **70**. These results could not be evaluated in terms of a general trend, however, because enediyne **68** failed to produce cyclized product (**77**). From the results, it was unclear if this lack of reactivity was due to the deactivating nature of the added aromatic ring in enediyne **68** or a result of the largest *cd* calculated for all the enediynes studied.

In accordance with the results in the photochemical study completed by Turro and Evenzahav,¹¹ it is postulated that the more rigid phenyl rings provided a more attainable singlet state of excitation over a triplet. The triplet state would lead to photo reduced products, which were not observed. Photo reduced products for the TMS substituted enediynes were observed on the GC-MS, however, they were not isolated or characterized due to their very low yields. This trend did not continue for the photochemical cyclizations of the TMS and Ph substituted quinoxaline starting materials. It was expected that the Ph enediyne would have a higher percent yield due to the rigidity of the phenyl substitution, however, it did not produce any of the desired cyclized product. It was concluded that the electronic state of the nitrogenous portion of the

phenyl enediyne (**68**) changed the nature of the singlet state, and as a result the compound was not as reactive as the TMS enediyne (**67**).

Table 5 - Calculated *cd* for Synthesized Enediynes

Enediyne	R	<i>cd</i> Ground State (Å) ^a	<i>cd</i> Excited State (Å) ^b
	TMS (65)	4.067-4.088	3.889
	C(CH ₃) ₂ OH (59)	4.085	4.119
	Ph (66)	4.063-4.067	3.637
	H (62)	4.066-4.090	3.901
	TMS (67)	3.349-4.051	4.070
	C(CH ₃) ₂ OH (61)	4.072	3.696
	Ph (68)	4.091-4.137	4.302
	H (64)	3.959-4.046	4.046
	TMS (69)	4.065-4.072	4.120
	C(CH ₃) ₂ OH (60)	4.078	4.120
	Ph (70)	4.040-4.059	3.869
	H (63)	4.025-4.082	3.838

^a MM2, MOPAC, ^b MOPAC

By examination of the *cd* calculated for the excited singlet states listed for the compounds in Table 5, it was observed that all of the distances are higher than the thermal stability limit of 25°C. All compounds were subjected to energy minimization calculations for the singlet state,

since this was the state that is proposed as the transition state for photochemical reactions.

Ground state calculations are also included in Table 5, because Nicolaou's evidence for thermal reactivity was based on the ground state *cd* values that were calculated and observed using X-ray structures. There is no trend, however, to explain, in terms of *cd*, why the deprotected enediynes (**62** and **64**) could thermally cyclize, while their hindered counterparts could not, since the estimated *cd* were close in value.

The photoreactive TMS- and phenyl-substituted enediynes had estimated *cd* between 3.889 and 4.302 Å. The *cd* range for compounds that did not cyclize was more difficult to interpret. All of the 3-methyl-3-hydroxy-substituted enediynes (**59**, **61**, **60**) had calculated *cd* between 3.696 and 4.120 Å, although, they were closer to the upper limit of the range. It was unclear if their lack of reactivity was due to their larger *cd*, poor solubility, less reactive singlet state, or a combination of these factors. It was surprising that the H-substituted enediyne (**62**) with a calculated *cd* of 3.901 Å did not photochemically cyclize, since this value falls in the middle of the *cd* range for successful cyclizations for the TMS and phenyl substituted pyridine enediynes. Similar to the 3-methyl-3-hydroxy-substituted enediynes, it was concluded that H-substitution must have altered the nature of the singlet state, rendering it less reactive. The lack of reactivity may be a factor of the non-rigid acetylenic units, thus reducing the quantum yield. Additionally, unlike the thermal reactions, the data suggested that the reaction energy required for the photochemical cyclization was not dependent on the *cd*.

3.3.2 Conclusion

The nature of the cyclization reactions of nitrogenous aromatic enediynes was investigated

through thermal and photochemical reactions. It was observed that thermal reactions did not proceed for the hindered enediynes as reported in the literature for the unhindered analogues. This was attributed to the steric demands of the alkynyl substituents. Photochemical reactions did proceed, however, with low yields. The percent yield trends suggested an inverse relationship with steric demand of the alkynyl substituents. It was concluded that the more important factor in photochemical reactivity is rigidity of the alkynyl substituents. This result agrees with those reported in the literature. Additionally, photoreduction was not observed for the phenyl substituted enediynes, while it was observed in the TMS substituted reactions. Calculations coupled with experimental evidence also questions the validity of the *cd* distance as a predictor of potential cyclization. The thermal stability of the nitrogenous enediynes coupled with their photoreactivity make them a good candidate for cell line trials used in conjunction with photodynamic techniques. Future work should include optimization of the photochemical reaction and toxicity studies.

CHAPTER FOUR

EXPERIMENTAL

4.1 General Experimental Techniques, Instrumentation and Materials

All experiments were performed in flame-dried flasks under positive pressure of N_2 unless otherwise stated in the procedure. Coupling reactions were performed in 15 mL Ace pressure tubes, flame-dried under N_2 . Thermal cyclizations were performed in 38 mL Ace pressure tubes which had been flame-dried under N_2 . Photochemical cyclizations were performed in quartz tubes flame-dried under N_2 and irradiated with a Hanovia 200 W medium pressure Hg arc lamp at $25 \pm 1^\circ C$. Liquid, moisture and air sensitive reagents were introduced to reaction mixtures through rubber septa using a syringe. All reactions were completed under inert atmospheres of nitrogen or argon, and all yields reported are isolated yields unless otherwise stated.

Solvents used for experiments were subjected to drying prior to use. Specifically, tetrahydrofuran (THF) was distilled from potassium, dichloromethane (CH_2Cl_2) was dried over molecular sieves for six hours, triethylamine (Et_3N) and diisopropylamine ($(iPr)_2NH$) were dried over calcium hydride and distilled from P_2O_5 as was carbon tetrachloride (CCl_4). Reaction progress was monitored using analytical thin layer chromatography (TLC) and gas-chromatography (GLC).

TLC was performed on silica gel of 5-17 μm particle size, 60 \AA pore size and a thickness of 250 μm with a 254 nm fluorescent indicator. Preparative TLC was performed on 150 \AA silica

gel plates of 1000 μm thickness. The solvents used are reported in parentheses and the concentrations were calculated by volume. Visualization of spots was achieved by viewing under UV light. GLC was performed on a Hewlett Packard 5890 equipped with a flame ionization detector (FID) using a 30 m by 0.25 mm DB-5HT column composed of (%5 phenyl) methylpolysiloxane. The carrier gas was nitrogen with a flow rate of 2.0 mL/min. Gas chromatography-mass spectrometry (GC-MS) was used to identify the mass of GC peaks. GC-MS was performed on a Hewlett Packard 5890 series II gas chromatograph equipped with a DB-5HT column and helium as the carrier gas. This system had a linear velocity of 35 cm/s. The GC was fitted to a VG Micromass Autospec mass spectrometer with a range of 52 to 510 mass units and a resolution of 3000 at an ionizing energy of 70 eV. Mass spectral data are reported as follows: parent ion (relative intensity), m/e of significant fragments (relative intensity).

Excess solvents were removed *in vacuo* on a Buchi rotary evaporator at pressures obtained by a water aspirator. All crude samples and purified compounds were stored in a freezer under nitrogen at -10°C . Reaction mixtures were purified by liquid chromatography. Separation was attained using 70 - 230 mesh silica gel, treated with approximately 1 mL of triethylamine. The solvent system used for separation was determined by analytical TLC. Often purity was obtained using a Harrison research chromatotron following flash chromatography. Chromatotron plates of 1mm and 2mm were used depending on the weight of crude material and composed of TLC grade silica gel mesh 5-40 μm with a gypsum binder and fluorescent indicator.

Proton nuclear magnetic resonance (^1H NMR) spectra were obtained on a Varian Unity Inova 500 MHz NMR at room temperature. Deuterated chloroform (CDCl_3) was the solvent used with an internal standard of 1% tetramethylsilane (TMS). Chemical shift values are

reported in parts per million (ppm) in the form: chemical shift (multiplicity, coupling constant in Hz, integration). ^{13}C NMR spectra were obtained on the same instrument, using the same solvent. CDCl_3 (δ 77.0) was used as the internal standard, with values reported in ppm downfield from TMS.

Infrared spectra were collected on a Bruker IFS Fourier transform infrared (FTIR) spectrophotometer. Spectra of liquid compounds were measured neat on NaCl plates, while solid compounds were measured as KBr discs. The data are reported for significant peaks in reciprocal centimetres. Ultraviolet spectra were recorded for all enediynes on a Perkin-Elmer Lambda 11 spectrometer, in CH_2Cl_2 . Wavelengths of significant peaks are reported as their maximum absorption in nanometers with their corresponding molar absorptivities (ϵ). Elemental analysis were recorded on a CEC 240-XA elemental analyser and are reported as percentages by weight.

Competitive rate reactions were monitored by High Pressure Liquid Chromatography using a Varian Prostar HPLC equipped with a 410 model autosampler, PDA detector and a 220/230/240 solvent delivery module. The solvent system used was dependant on the identity of the compounds to be separated and was conducted on a 25 cm Chromspher 5 C8 or a 25 cm Zorbax SB-C18 high performance column.

Tetrakis(triphenylphosphine)palladium(0) was synthesized using a published procedure and was stored in the freezer.^a Compounds **38** and **46** were prepared as in literature references and were compared to the values contained within those references. All compounds without a supplied procedure were purchased from Aldrich.

4.2 Preparations

4.2.1 Procedures for the Preparation of Starting Materials

2,3-Di(trifluoromethylsulfonyl)pyridine (35). 2,3-Dihydroxy pyridine (246 mg, 2.21 mmol) was dissolved in dry pyridine (7.0 mL) in a round bottom flask. The solution was cooled to 0°C under an N₂ atmosphere. Trifluoromethane sulfonic anhydride (0.83 mL, 4.9 mmol) was added dropwise over 30 minutes. The solution was allowed to warm to room temperature and stirred under N₂ for 3 days. The reaction was quenched with cold water (10.0 mL) and extracted three times with CH₂Cl₂ (10 mL). The organic extracts were washed three times with equal volumes of water, 10% HCl, water, brine and dried over MgSO₄. Volatile solvents were removed with rotary evaporation under reduced pressure. The black oily residue was subjected to column chromatography to give a yellow oil (665 mg, 80%).

TLC (20% EtOAc in hexanes): R_f = 0.39; IR (neat): 3087, 2360, 1436, 1221, 1092; ¹H NMR (CDCl₃): δ 8.41 (m, 1H), 7.90 (dt, J = 8, 2 Hz, 1H), 7.52 (dd, J = 13, 5 Hz, 1H); ¹³C NMR (CDCl₃): δ 147.3, 147.2, 135.6, 133.7, 125.4, 118.5; MS: 375 (M⁺, 45), 279 (20), 214(60), 149 (100)

2,3-Di(methanesulfonyl)pyridine (36). 2,3-dihydroxy pyridine (337 mg, 3.0 mmol) and DMAP (18.4 mg, 0.15 mmol) were dissolved in dry CH₂Cl₂ (10.0 mL) and TMEDA (1.36 mL, 9.0 mmol) in a round bottom flask. The solution was cooled to 0°C under an N₂ atmosphere. Methanesulfonyl chloride (0.40 mL, 4.6 mmol) was added dropwise. The solution was stirred

under N₂ at 0°C for 4 hours. Excess methanesulfonyl chloride was decomposed with addition of TMEDA (0.08 mL, 0.5 mmol). The reaction was quenched with cold water (10.0 mL) and extracted four times with CH₂Cl₂ (10 mL). The organic extracts were washed once with equal volumes of water, brine and dried over MgSO₄. Volatile solvents were removed with rotary evaporation under reduced pressure. The brown oily residue was subjected to column chromatography to give a pale yellow crystal after subjecting to reduced pressure (463 mg, 58%). TLC (30% EtOAc in hexanes): R_f = 0.14; IR (KBr): 3036, 2941, 1675, 1438, 1366, 1178; ¹H NMR (CDCl₃): δ 8.20 (m, 1H), 7.79 (m, 1H), 7.31 (m, 1H), 3.52 (s, 3H), 3.27 (s, 3H); ¹³C NMR (CDCl₃): δ 149.7, 146.0, 136.2, 134.9, 124.1, 41.6, 39.2; MS: 267 (M⁺, 10), 188 (27), 160 (40), 82 (100); CHN (C₇H₉NO₆S₂): Calculated: C 31.46, H 3.40, N 5.24; Found: C 31.26, H 3.29, N 5.16.

2-bromo-3-trifluoromethanesulfonylpyridinate (38).³² 2-Bromo-3-pyridinol (1.02 g, 5.84 mmol) was dissolved in CH₂Cl₂ (15.0 mL) in a round bottom flask. The flask was purged with Ar as it was cooled to 0°C in a ice/salt/water bath. Trifluoromethanesulfonyl anhydride (1.21 mL, 7.20 mmol) was added dropwise via syringe over 15 minutes with stirring. The solution was allowed to warm to room temperature and stirred overnight. The volatile solvents were removed by rotary evaporation under reduced pressure. The residue was purified by column chromatography to give a yellow oil (1.69 g, 95%).

TLC (30% EtOAc in hexanes); R_f = 0.54; ¹H NMR (CDCl₃): δ 8.41 (dd, *J* = 5, 2 Hz, 1H), 7.68 (dd, *J* = 8, 2 Hz, 1H), 7.40 (dd, *J* = 8, 5 Hz, 1H); ¹³C NMR (CDCl₃): δ 149.9, 145.0, 136.1, 131.0, 124.2, 117.5; MS: 305 (M⁺ 35), 144 (35), 96 (100)

2-bromo-3-methanesulfonylpyridinate (37). 2-Bromo-3-pyridinol (1.02 g, 5.83 mmol) was dissolved in CH_2Cl_2 (15.0 mL) in a one neck 50 mL round bottom flask. DMAP (44.5 mg, 0.36 mmol) and TMEDA (2.2 mL, 18.0 mmol) were added. The flask was purged with Ar as it was cooled to 0°C in a ice/salt/water bath. Methanesulfonyl chloride (0.70 mL, 9.0 mmol) was added dropwise via syringe over 10 minutes while stirring. The solution was allowed to warm to room temperature and stirred overnight. The volatile solvents were removed by rotary evaporation under reduced pressure. The residue was purified by column chromatography to give a yellow oil (1.23 g, 84%).

TLC (30% EtOAc in hexanes): $R_f = 0.30$; IR (neat): 3031, 2937, 1732, 1567, 1445, 1375, 1175 ^1H NMR (CDCl_3): δ 8.31 (m, 1H), 7.72 (m, 1H), 7.33 (m, 1H), (s, 3H); ^{13}C NMR (CDCl_3): δ 148.3, 144.1, 136.0, 132.4, 124.1, 39.6; MS 251 (M^+ , 55), 172 (100), 144(60)

3-chloro-2-trifluoromethanesulfonylpyridinate (53).³² 2-Chloro-3-pyridinol (1.01 g, 7.72 mmol) was dissolved in CH_2Cl_2 (15.0 mL) in a round bottom flask. The flask was purged with Ar as it was cooled to 0°C in a ice/salt/water bath. Trifluoromethanesulfonyl anhydride (1.21 mL, 7.20 mmol) was added dropwise via syringe over 15 minutes with stirring and argon purge. The solution was allowed to warm to room temperature and stirred overnight. The volatile solvents were removed by rotary evaporation under reduced pressure. The residue was purified by column chromatography to give a yellow oil (2.02 g, 99%).

TLC (30% EtOAc in hexanes); $R_f = 0.46$; ^1H NMR (CDCl_3): δ 8.43 (s, 1H), 7.71 (m, 1H), 7.38 (m, 1H); ^{13}C NMR (CDCl_3): δ 148.9, 144.5, 143.0, 131.5, 123.9, 117.4; MS: 260 (M^+ 65), 197 (45), 93 (100)

2-Cyanoaziridine (46).⁷⁰ Methanol (18.0 mL) was stirred in an one-necked 100 mL round bottom flask and cooled to 0°C in an ice/salt/water bath. The MeOH was saturated with NH₃ over an hour, and 2,3-dibromopropionitrile (2.34 mL, 23.0 mmol) was added dropwise over twenty minutes, via syringe. The mixture was stirred at 0°C for one hour and then allowed to warm to room temperature. Triethanolamine (6.1 mL, 46 mmol) was added and the solution was refluxed for four hours and stored in the freezer overnight. The solution was vacuum filtered, and washed with 1 M H₂SO₄ (2 mL), saturated NaHCO₃ (10 mL), and then extracted with ethyl acetate (15 mL, 5 times). The solvent was removed by rotary evaporation. Product was vacuum distilled at 50°C and 0.2 Torr, to give a clear, colourless oil (271 mg, 17%)
¹H NMR (CDCl₃): δ 2.44 (m, 1H), 2.12 (m, 2H), 0.99 (broad s, 1H); ¹³C NMR (CDCl₃): δ 119.7, 25.8, 25.2 (invertomere), 15.0, 14.2.

General Procedure for Esterification of Iodobenzoic Acids

A three-necked round bottom flask, equipped with a magnetic stir-bar was flame-dried under nitrogen. 3- or 4-iodobenzoic acid (2.5 - 8.0 mmol) was added to the flask and thionyl chloride (0.22 - 0.7 mL, 3 - 9.6 mmol) was added dropwise via syringe over thirty minutes. The mixture was refluxed at 80°C for 50 minutes and then cooled below 25°C in an ice/water bath. Anhydrous alcohol was then added dropwise via syringe and the mixture was refluxed at 80°C for 30 minutes. The reaction was quenched with 20 mL of ice water and frozen overnight. The mixture was extracted three times with ether (30 mL), and washed with saturated NaHCO₃ (20 mL), and saturated NaCl (20 mL). The organic extracts were dried over MgSO₄, filtered and excess solvent removed with rotary evaporation. Purity was assessed using GC and ¹H NMR.

Methyl-3-iodobenzoate(54)

3-iodobenzoic acid (2.0 g, 8.0 mmol), thionyl chloride (0.7 mL, 9.6 mmol), methanol (1.6 mL, 38 mmol). Product was isolated as a yellow oil (1.3 g, 63%)

^1H NMR (CDCl_3): δ 8.13 (t, $J = 1.5$ Hz, 1H), 7.75 (dd, $J = 6.5, 1.0$ Hz, 1H), 7.63 (dd, $J = 6.5, 1.0$ Hz, 1H), 7.00 (s, 1H), 3.68 (s, 3H); ^{13}C NMR (CDCl_3): δ 165.9, 141.9, 138.6, 132.0, 128.9, 93.4, 52.5; MS: 262 (M^+ , 99%), 231 (100), 203 (75), 76 (73)

Methyl-4-iodobenzoate (55)

4-iodobenzoic acid (1.3 g, 5.4 mmol), thionyl chloride (0.54 mL, 6.4 mmol), methanol (1.3 mL, 30 mmol). Product was isolated as a yellow crystalline solid (0.58 g, 42%)

^1H NMR (CDCl_3): δ 7.90 (dt, $J = 8.5, 2.0$ Hz, 2H), 7.74 (dt, 8.5, 2.0 Hz, 2H), 3.91 (s, 3H); ^{13}C NMR (CDCl_3): δ 180.2, 138.5, 137.9, 137.8, 131.9, 52.4; MS: 262 (M^+ , 90%), 231 (100), 203 (70), 76 (75)

Ethyl-3-iodobenzoate (56)

3-iodobenzoic acid (0.61 g, 2.5 mmol), thionyl chloride (0.22 mL, 3.0 mmol), ethanol (0.69 mL, 12 mmol). Product was isolated as a yellow/brown oil (0.59 g, 86%)

^1H NMR (CDCl_3): δ 8.37 (s, 1H), 8.00 (d, 1H), 7.86 (d, 1H), 7.17 (t, 1 H), 4.36 (quart, 2 H), 1.39 (t, 3 H); ^{13}C NMR (CDCl_3): δ 165.1, 141.7, 138.5, 132.5, 130.1, 128.8, 93.1, 61.5, 14.4; MS: 275 (M^+ , 85%), 247 (80), 231 (100), 203 (65), 76 (80)

Ethyl-4-iodobenzoate (57)

4-iodobenzoic acid (0.61 g, 2.5 mmol), thionyl chloride (0.22 mL, 3.0 mmol), ethanol (0.69 mL, 12 mmol). Product was isolated as a yellow oil (0.35 g, 50%)

^1H NMR (CDCl_3): δ 7.77 (dd, $J = 15.5, 9.0$ Hz, 4H), 4.36 (q, $J = 7.0$ Hz, 2H), 1.38 (t, $J = 7.0, 3\text{H}$); ^{13}C NMR (CDCl_3): δ 166.2, 137.8, 131.1, 130.1, 61.4, 14.4; MS: 276 (M^+ , 80%), 248 (85), 231 (100), 203 (70), 76 (75)

4.2.2 Procedures for Songashira Coupling Reactions

3-chloro-2-trimethylsilylethynylpyridine.³² A 15 mL Ace pressure tube was charged with diisopropylamine (13.0 mL) and degassed with Ar bubbling for 10 minutes. $\text{Pd}(\text{PPh}_3)_4$ (53 mg, 0.05 mmol), 2,3-dichloropyridine (503 mg, 3.4 mmol), and trimethylsilylacetylene (1.2 mL, 8.5 mmol) were added and the tube was sealed. The solution was stirred at 170°C for 13 hours. The solution was filtered through a silica plug (1:9 EtOAc:hexane). The product was isolated via column chromatography followed by a chromatatron as a pale yellow oil (346 mg, 49%).

TLC (10% EtOAc in hexanes) $R_f = 0.39$; IR (neat); ^1H NMR (CDCl_3): δ 8.45 (m, 1H); 7.70 (m, 1H); 7.19 (m, 1H); 0.29 (s, 9H); ^{13}C NMR (CDCl_3): δ 147.8, 141.8, 138.9, 136.8, 123.8, 101.3, 100.4, 0; MS: 209 (M^+ , 55), 194 (100), 130 (20), 63 (22) .

2,3-bis-(trimethylsilylethynyl)pyridine (65).³² A 40 mL Ace pressure tube was charged with diisopropylamine (20 mL) and degassed with Ar bubbling for 10 minutes. $\text{Pd}(\text{PPh}_3)_4$ (64.4mg, 0.04 mmol) CuI (67.7 mg, 0.40 mmol), 2-bromo-3-trifluoromethanesulfonylpyridine (620.7 mg,

2.04 mmol), and trimethylsilylacetylene (0.96 mL, 6.8 mmol) were added and the tube was sealed. The solution was stirred at 100°C for 13 hours. The solution was filtered through a silica plug (1:9 EtOAc:hexane). The product was isolated via column chromatography as a dark yellow oil (410.9 mg, 74%).

TLC (15% EtOAc in hexanes) R_f = 0.41; IR (neat): 2961, 2899, 2166, 1544; UV (CH_2Cl_2): λ_{max} = 264 (ϵ = 24000), 270 (25000), 276 (24000); ^1H NMR (CDCl_3): δ 8.45 (d, J = 5 Hz, 1H); 7.71 (d, J = 8 Hz, 1H); 7.14 (dd, J = 8, 5 Hz, 1H); 0.26 (s, 9H); 0.25 (s, 9H); ^{13}C NMR (CDCl_3): δ 148.8, 144.8, 139.5, 122.8, 122.2, 102.2, 101.9, 100.8, 99.2, 0; MS: 271 (M^+ , 25) 256 (100), 212 (7), 73 (93).

2,3-bis-(2-methyl-3-butyn-2-ol)pyridine (59).³² A 40 mL Ace pressure tube was charged with diisopropylamine (20.0 mL) and degassed with Ar bubbling for 10 minutes. $\text{Pd}(\text{PPh}_3)_4$ (58.9 mg, 0.05 mmol), CuI (56.7 mg, 0.30 mmol), 2-bromo-3-trifluoromethanesulfonylpyridine (597.6 mg, 1.96 mmol), and 2-methyl-3-butyn-2-ol (0.48 mL, 5.0 mmol) were added and the tube was sealed. The solution was stirred at 100°C for 18 hours. The solution was filtered through a silica plug (1:1 EtOAc:hexane). The product was isolated via flash chromatography as a yellow solid (362.9 mg, 76%).

TLC (50% EtOAc in hexanes); R_f = 0.11; IR (KBr): 3355, 2977, 2927, 2236, 1422, 1168; UV (CH_2Cl_2): λ_{max} = 256 (ϵ = 23000), 260 (28000), 268 (25000); ^1H NMR (CDCl_3): δ 8.16 (m, 1H); 7.40 (m, 1H); 6.92 (m, 1H); 4.29 (broad s, 2H); 1.33 (m, 12H); ^{13}C NMR (CDCl_3): δ 144.6, 138.0, 122.5, 121.7, 121.6, 101.1, 98.3, 79.6, 77.6, 64.6, 64.5 30.8, 30.7; MS: 243 (M^+ , 25) 210 (100), 200 (25), 183 (20), 167 (55).

CHN calculated (C₁₅NO₂H₁₇): C 74.03, H 7.05, N 5.76; Found: C 74.01, H 7.36, N 5.26.

2,3-bis-(phenylethynyl)pyridine (66).³² A 15 mL Ace pressure tube was charged with diisopropylamine (10.0 mL) and degassed with Ar bubbling for 10 minutes. Pd(PPh₃)₄ (34.5 mg, 0.03 mmol), CuI (34.2 mg, 0.18 mmol), triphenylphosphine (65.3 mg, 0.25 mmol), 2-bromo-3-trifluoromethanesulfonylpyridine (330.6 mg, 1.08 mmol), and phenylacetylene (0.40 mL, 3.64 mmol) were added and the tube was sealed. The solution was stirred at 100°C for 13 hours. The solution was filtered through a silica plug (1:9 EtOAc:hexane). The product was isolated from flash chromatography as a brown oil (121.2 mg, 40%).

TLC (10% EtOAc in hexanes): R_f = 0.11; IR (neat): 3056, 2361, 2219, 1492, 1420; UV (CH₂Cl₂): λ_{max} = 272 (ε = 32000), 276 (28000), 311 (22000); ¹H NMR (CDCl₃): δ 8.54 (m, 1H); 7.83 (m, 1H); 7.63 (m, 2H); 7.58 (m, 2H); 7.36 (m, 6H); 7.22 (m, 1H); ¹³C NMR (CDCl₃): δ 148.8, 145.1, 138.9, 132.2, 131.8, 129.2, 129.0, 128.6, 123.1, 122.7, 122.4, 122.1, 96.2, 93.5, 88.0, 85.1; MS: 279 (M⁺, 100) 250 (11), 150 (6), 139 (14), 76 (5).

2,3-bis-(trimethylsilylethynyl)quinoxaline (67).³² A 40 mL Ace pressure tube was charged with diisopropylamine (20.0 mL) and degassed with Ar bubbling for 10 minutes. Pd(PPh₃)₄ (81.2 mg, 0.07 mmol), CuI (87.6 mg, 0.46 mmol), 2,3-dichloroquinoxaline (800.0 mg, 4.02 mmol) and trimethylsilylacetylene (1.70 mL, 12.0 mmol) were added and the tube was sealed. The solution was stirred at 100°C for 18 hours. The solution was filtered through a silica plug and charcoal plug (10% EtOAc in hexane). The product was isolated using flash chromatography followed by rotary chromatography as a yellow solid (530.9 mg, 40%).

TLC (10% EtOAc in hexanes): $R_f = 0.41$; IR (KBr): 2957, 2899, 2162, 1328, 1248; UV (CH_2Cl_2): $\lambda_{\text{max}} = 264$ ($\epsilon = 124000$), 268 (159000), 271 (140000), 356 (32000), 373 (40000); ^1H NMR (CDCl_3): δ 8.02 (m, 2H); 7.73 (m, 2H); 0.33 (s, 18H); ^{13}C NMR (CDCl_3): δ 140.5, 140.3, 131.2, 129.0, 102.4, 100.9, 0; MS: 322 (M^+ , 70), 307 (100), 263 (6), 146 (19), 73 (75); CHN calculated ($\text{C}_{18}\text{N}_2\text{Si}_2\text{H}_{22}$): C 67.08, H 6.83, N 8.69; Found: C 66.34, H 6.58, N 8.20.

2,3-bis-(2-methyl-3-butyn-2-ol)quinoxaline (61).³² A 15 mL Ace pressure tube was charged with diisopropylamine (7.0 mL) and degassed with Ar bubbling for 10 minutes. $\text{Pd}(\text{PPh}_3)_4$ 23 mg, 0.02 mmol), CuI (20 mg, 0.11 mmol), 2,3-dichloroquinoxaline (202mg, 1.01 mmol) and 2-methyl-3-butyn-2-ol (0.24 mL, 2.5 mmol) were added and the tube was sealed. The solution was stirred at 80°C for 13 hours. The solution was filtered through a silica plug and charcoal plug (100% EtOAc). The product was isolated using flash chromatography as a white solid (229mg, 77%).

TLC (50% EtOAc in hexanes): $R_f = 0.30$; IR (KBr): 2981, 2931, 2224, 1634, 1341; UV (CH_2Cl_2): $\lambda_{\text{max}} = 264$ ($\epsilon = 70000$), 268 (68000), 351 (20000), 368 (24000); ^1H NMR (CDCl_3): δ 8.01 ppm (m, 2H); 7.72 ppm (m, 2H); 4.42 ppm (broad s, 2H); 1.70 ppm (s, 12H); ^{13}C NMR (CDCl_3): δ 140.7, 140.3, 131.1, 129.0, 101.2, 79.6, 65.9, 31.1; MS: 294 (M^+ , 35), 279 (85), 261 (100), 251 (45), 234 (25), 218 (40); CHN calculated ($\text{C}_{18}\text{O}_2\text{N}_2\text{H}_{18}$): C 73.45 H 6.16 N 9.52; Found: C 73.10, H 6.30, N 9.00.

2,3-bis-(phenylethynyl)quinoxaline (68).³² A 15 mL Ace pressure tube was charged with diisopropylamine (5.0 mL) and degassed with Ar bubbling for 10 minutes. $\text{Pd}(\text{PPh}_3)_4$ (19 mg,

0.02 mmol), CuI (21mg, 0.11 mmol), 2,3-dichloroquinoxaline (210 mg, 1.05 mmol) and phenylacetylene (0.27 mL, 2.5 mmol) were added and the tube was sealed. The solution was stirred at 80°C for 18 hours. The solution was filtered through a silica plug and charcoal plug (10% EtOAc in hexane). The product was isolated using flash chromatography as a brown solid (64 mg, 17%).

TLC (10% EtOAc in hexanes): $R_f = 0.34$; IR (KBr): 2922, 2851, 2202, 1353, 1121; UV (CH_2Cl_2): $\lambda_{max} = 263$ ($\epsilon = 56000$), 287 (80000), 296 (70000), 301 (64000), 384 (24000); ^1H NMR (CDCl_3): δ 8.07 (m, 2H); 7.75 (m, 2H); 7.69 (m, 4H); 7.39 (m, 6H); ^{13}C NMR (CDCl_3): δ 141.0, 140.6, 132.5, 131.0, 130.0, 129.0, 128.7, 121.7, 96.0, 86.9; MS: 330 (M^+ , 100), 203 (60), 165 (25), 127 (25), 76 (20); CHN calculated ($\text{C}_{24}\text{N}_2\text{H}_{14}$): C 87.3, H 4.24, N 8.48; Found: C 63.7, H 6.68, N 8.06.

2,3-bis-(trimethylsilylethynyl)pyrazine (69).³² A 15 mL Ace pressure tube was charged with diisopropylamine (10.0 mL) and degassed with Ar bubbling for 10 minutes. $\text{Pd}(\text{PPh}_3)_4$ (36.6 mg, 0.03 mmol), CuI (33.6 mg, 0.18 mmol), 2,3-dichloropyrazine (0.21 mL, 2.02 mmol) and trimethylsilylacetylene (1.00 mL, 7.08 mmol) were added and the tube was sealed. The solution was stirred at 115°C for 18 hours. Solution was filtered through a silica and charcoal plug (1:9 EtOAc:hexanes). Product was isolated using flash chromatography followed by rotary chromatography as a yellow oil (407.9 mg, 74 %).

TLC (10% EtOAc in hexanes): $R_f = 0.29$; IR (neat): 2961, 2899, 2170, 1519, 1370, 1249; UV (CH_2Cl_2): $\lambda_{max} = 265$ ($\epsilon = 20000$), 281 (18000), 305 (12000), 326 (10000); ^1H NMR (CDCl_3): δ 8.40 (s, 2H); 0.27 (s, 18H); ^{13}C NMR (CDCl_3): δ 142.5, 141.4, 103.0, 100.2, 0; MS: 272 (M^+ ,

30), 257 (100), 108 (15), 73 (95).

2,3-bis-(2-methyl-3-butyn-2-ol)pyrazine (60).³² A 15 mL Ace pressure tube was charged with diisopropylamine (5.0 mL) and degassed with Ar bubbling for 10 minutes. Pd(PPh₃)₄ (15 mg, 0.01 mmol), CuI (19 mg, 0.10 mmol), 2,3-dichloropyrazine (0.10 mL, 0.96 mmol) and 2-methyl-3-butyn-2-ol (0.34 mL, 3.5 mmol) were added and the tube was sealed. The solution was stirred at 120°C for 18 hours. Solution was filtered through a silica plug and charcoal plug (1:1 EtOAc:hexanes). Product was isolated, using flash chromatography, as a pale yellow solid (178 mg, 76%).

TLC (50% EtOAc in hexanes): R_f = 0.16; IR (KBr): 2983, 2932, 2233, 1397, 1155; UV (CH₂Cl₂): λ_{max} = 256 (ε = 12500), 264 (14000), 268 (12000), 303 (10000), 312 (9500), 316 (9500); ¹H NMR (CDCl₃): δ 8.39 (s, 2H); 4.34 (broad s, 2H); 1.64 (s, 12H); ¹³C NMR (CDCl₃): δ 142.3, 141.7, 101.6, 78.6, 65.6, 31.0; MS: 244 (M⁺, 15), 229 (42), 211 (100), 201 (30), 183 (45), 169 (37); CHN calculated (C₁₄N₂O₂H₁₆): C 68.82, H 6.61, N 11.47. Found: C 66.11, H 6.57, N 9.93.

2,3-bis-(phenylethynyl)pyrazine (70).³² A 15 mL Ace pressure tube was charged with diisopropylamine (6.0 mL) and degassed with Ar bubbling for 10 minutes. Pd(PPh₃)₄ (17 mg, 10%), CuI (16 mg, 10%), 2,3-dichloropyrazine (0.11 mL, 1.1 mmol) and phenylacetylene (0.35 mL, 3.2 mmol) were added and the tube was sealed. The solution was stirred at 100°C for 13 hours. Solution was filtered through a silica plug and charcoal plug (1:9 EtOAc:hexanes). The product was isolated, using flash chromatography, as a pale yellow solid (138 mg, 52%).

TLC (10% EtOAc in hexanes): $R_f = 0.11$; IR (KBr): 3047, 2923, 2201, 1596, 1491, 1369; UV (CH_2Cl_2): $\lambda_{\text{max}} = 312$ ($\epsilon = 44000$), 320 (40000), 326 (44000); ^1H NMR (CDCl_3): δ 8.48 (s, 2H); 7.64 (m, 4H); 7.37 (m, 6H); ^{13}C NMR (CDCl_3): δ 142.4, 142.0, 132.3, 129.8, 128.6, 121.8, 96.4, 86.1; MS: 280 (M^+ , 100), 253 (10), 207 (6), 140 (15), 127 (99), 75 (7); CHN calculated ($\text{C}_{20}\text{N}_2\text{H}_{12}$): C 85.69, H 4.32, N 10.00; Found: C 85.10, H 5.10, N 8.94.

4.2.3 Procedures for Alkynyl Deprotections

General Procedure for Alkynyl Deprotections

A 25 mL round bottom flask was equipped with a magnetic stir-bar and flame-dried under N_2 . The flask was charged with 4 mL toluene, 0.5 - 1 mmol enediyne and 15 mg NaH. The solution was refluxed for one hour and then half of the toluene was distilled from the reaction mixture. The solution was filtered and the solvent was removed under reduced pressure. The crude solid was diluted in 20 mL CH_2Cl_2 and washed one time with 10 mL 5% NaHCO_3 and one time with 10 mL water. The organic layer was dried with MgSO_4 , filtered and the solvent was removed under reduced pressure. The product was isolated using column chromatography.

2,3-bis-ethynylpyridine (62)

Product was isolated as a yellow solid (51.3 mg, 52%).

TLC (10% EtOAc in hexanes): $R_f = 0.13$; ^1H NMR (CDCl_3): δ 8.50 (m, 1H), 7.76 (m, 1H), 7.22 (m, 1H), 3.44 (s, 1H), 3.38 (s, 1H); ^{13}C NMR (CDCl_3): δ 149.3, 144.4, 139.9, 122.7, 122.2, 84.2, 81.2, 81.1, 79.5; MS: 127 (M^+ , 100%), 101 (74), 74 (65).

2,3-bis-ethynylquinoxaline (64)

Product was isolated as a pale yellow solid (3.3 mg, 4%).

TLC (10% EtOAc in hexanes): $R_f = 0.17$; MS: 128 (M^+ , 100), 102 (22), 77 (24).

2,3-bis-ethynylpyrazine (63)

Product was isolated as a yellow solid (7.8 mg, 7%).

TLC (10% EtOAc in hexanes): $R_f = 0.15$; MS: 185 (M^+ , 100), 171 (7), 157 (18), 143 (10).

4.2.4 Procedures for Thermal Cyclizations

General Procedure for Thermal Cyclizations

A 38 mL Ace pressure tube was flame-dried under N_2 . The tube was charged with 20 mL CCl_4 and enediyne (0.10 mmol). The solution was degassed with Ar bubbling for 15 minutes. The tube was heated to 200°C until there was no visible change by TLC or GLC. Excess volatiles were removed with rotary evaporation. GC yields were calculated using a R_f^0 calculated for each enediyne using the formulas:

$$R_f^0 = (\text{Area enediyne} \times [\text{biphenyl}]) \div (\text{Area biphenyl} \times [\text{enediyne}])$$

$$[\text{cyclized}] = (\text{Area cyclized} \times [\text{biphenyl}]) \div (\text{Area biphenyl} \times R_f^0)$$

$$\% \text{ cyclized} = (\text{mole cyclized}) \div (\text{mole starting material}) \times 100\%$$

$$\% \text{ converted} = 100\% - [(\text{mole recovered starting material}) \div (\text{mole starting material}) \times 100\%]$$

2,5-dichloro-3,4-bis-(trimethylsilyl)phenazine (75)

2,3-bis-(trimethylsilylethynyl)quinoxaline (30.3 mg, 0.09 mmol). GC yield: 0 %.

2,5-dichloro-3,4-bis-(2-hydroxy-2-propyl)phenazine (76)

2,3-bis-(3-methyl-2-butyn-3-ol)quinoxaline (29.2 mg, 0.10 mmol). GC yield: 0 %.

2,5-dichloro-3,4-bis-(phenyl)phenazine (77)

Not attempted

2,5-dichloro-3,4-bis-(trimethylsilyl)quinoline (71)

2,3-bis-(trimethylsilylethynyl)pyridine (30.3 mg, 0.11 mmol). GC yield: 0 %.

2,5-dichloro-3,4-bis-(2-hydroxy-2-propyl)quinoline (72)

2,3-bis-(3-methyl-2-butyn-3-olethynyl)pyridine (23.5 mg, 0.10mmol). GC yield: 0 %.

2,5-dichloro-3,4-bis-(phenyl)quinoline (73)

2,3-bis-(phenylethynyl)pyridine (26.9 mg, 0.10 mmol). GC yield: 0 %.

2,5-dichloro-3,4-bis-(trimethylsilyl)quinoxaline (78)

2,3-bis-(trimethylsilylethynyl)pyrazine (27.4 mg, 0.10 mmol). Cyclized product 0 %.

2,5-dichloro-3,4-bis-(2-hydroxy-2-propyl)quinoxaline (79)

2,3-bis-(3-methyl-2-butyn-3-olethynyl)pyrazine (24.8 mg, 0.10 mmol). GC yield: 0 %.

2,5-dichloro-3,4-bis-(phenyl)quinoxaline (80)

2,3-bis-(phenylethynyl)pyrazine (29.8 mg, 0.11 mmol). GC yield: 0 %.

4.2.5 Procedures for Photochemical Cyclizations

General Procedure for Photochemical Cyclizations

A 40 mL quartz tube was flame-dried under N₂. The tube was charged with 20 mL CCl₄ and enediyne (0.10 mmol). The solution was degassed with Ar bubbling for 15 minutes. The tube was irradiated until there was no visible change by TLC or GLC. Excess solvents were removed with rotary evaporation. Purification was performed using rotary chromatography.

2,5-dichloro-3,4-bis-(trimethylsilyl)phenazine (75)

2,3-bis-(trimethylsilylethynyl)quinoxaline (32.3 mg, 0.10 mmol). GC yield: 2 %.

¹³C NMR (CDCl₃): δ 141.6, 131.8, 131.5, 131.2, 129.6, 129.3

2,5-dichloro-3,4-bis-(2-hydroxy-2-propyl)phenazine (76)

2,3-bis-(3-methyl-2-butyn-3-olethynyl)quinoxaline (29.8 mg, 0.10 mmol). GC yield: 0 %.

2,5-dichloro-3,4-bis-(phenyl)phenazine (77)

2,3-bis-(phenylethynyl)quinoxaline (33.2 mg, 0.10 mmol). GC yield: 0 %.

2,5-dichloro-3,4-bis-(trimethylsilyl)quinoline (71)

2,3-bis-(trimethylsilylethynyl)pyridine (29.2 mg, 0.11 mmol). GC yield: 1 %.

¹³C NMR spectrum. ¹H NMR spectrum to follow.

2,5-dichloro-3,4-bis-(2-hydroxy-2-propyl)quinoline (72)

2,3-bis-(3-methyl-2-butyn-3-olethynyl)pyridine (25.6 mg, 0.11 mmol). GC yield: 0 %.

2,5-dichloro-3,4-bis-(phenyl)quinoline (73)

2,3-bis-(phenylethynyl)pyridine (29 mg, 0.10 mmol). GC yield: 4%

¹³C NMR (CDCl₃): δ 171.3, 149.2, 132.9, 132.5, 132.4, 132.1, 131.9, 130.9, 130.4, 129.9, 129.5, 128.8, 128.6, 128.5, 128.4, 128.3, 127.4, 127.1, 121.5

2,5-dichloroquinoline (74)

2,3-bis-ethynylpyridine (13.1 mg, 0.10 mmol). GC yield: 0 %.

2,5-dichloro-3,4-bis-(trimethylsilyl)quinoxaline (78)

2,3-bis-(trimethylsilyl)pyrazine (mg, 0.10 mmol). GC yield: 2%

¹H NMR (CDCl₃): δ 8.40 (d, J = 2.5 Hz, 1H), 8.29 (d, J = 3.0 Hz, 1H), 0.51 (s, 9H), 0.44 (s, 9H);

¹³C NMR (CDCl₃): δ 151.2, 150.9, 147.0, 145.9, 142.4, 142.0, 140.8, 139.8, 1.3, 1.1

2,5-dichloro-3,4-bis-(2-hydroxy-2-propyl)quinoxaline (79)

2,3-bis-(3-methyl-2-butyn-3-olethynyl)pyrazine (24.9 mg, 0.10 mmol). GC yield: 0 %.

2,5-dichloro-3,4-bis-(phenyl)quinoxaline (80)

2,3-bis-(phenylethynyl)pyrazine (27.5 mg, 0.10 mmol). GC yield: 4%.

¹³C NMR (CDCl₃): δ 150.1, 150.0, 148.9, 148.7, 145.7, 145.5, 144.4, 144.3, 142.5, 142.4, 141.6, 141.4, 141.1, 140.9.

4.2.6 Procedures for Competitive Rate Reactions

General Procedure for Competitive Rate Reactions

A round bottom flask was flame dried under N₂ and charged with THF (2.5mL), biphenyl (1 mmol), iodobenzene (1 mmol), and 3 or 4-substituted iodobenzene (1 mmol). 7.5 μL was extracted and diluted in 0.5 mL MeOH. The solution was filtered through a 0.45 μm syringe disc filter and frozen. The round bottom was charged with triethylamine (0.21 mL), Pd(PPh₃)₄, (0.02 mmol), CuI (0.06 mmol) and trimethylsilylacetylene (1.1 mmol). Immediately following trimethylsilylacetylene addition a 7.5 μL sample was removed and treated as above. Samples were regularly extracted every 30 minutes after addition until no change was visible by HPLC. Once the experiment had been completed, the concentrations of the starting materials were calculated for each sample using the formula, $A_0/C_0 = A_x/C_x$, where A₀ and C₀ are the area and concentration in the initial sample. A_x and C_x represents the area and concentration of the in the half hour samples. HPLC methods used were previously determined (Table 5-11).

Table 6: Method of Separation for Iodoanilines

Time (min)	Flow Rate (mL/min)	%Acetonitrile	%H ₂ O
initial	1.1	40	60
5	1.1	40	60
30	1.1	55	45
35	1.1	100	0

Table 7: Method of Separation for Iodoanisoles

Time (min)	Flow Rate (mL/min)	%MeOH	%H ₂ O
initial	0.80	70	30
5	0.80	70	30
15	0.80	71	29
30	1.0	75	25
40	1.0	100	0

Table 8: Method of Separation for Iodobenzotrifluorides

Time (min)	Flow Rate (mL/min)	%Acetonitrile	%H ₂ O
initial	0.80	65	35
5	0.80	65	35
30	0.80	100	0
35	0.80	100	0

Table 9: Method of Separation for Iodoethylbenzene

Time (min)	Flow Rate (mL/min)	%Acetonitrile	%H ₂ O
initial	1.1	48	52
18	1.1	48	52
25	1.1	49	51
50	1.1	100	0

Table 10: Method of Separation for Iodonitrobenzenes

Time (min)	Flow Rate (mL/min)	%MeOH	%H ₂ O
initial	1.1	53	47
5	1.1	53	47
30	1.1	79	21
35	1.1	100	0

Table 11: Method of Separation for Iodophenols

Time (min)	Flow Rate (mL/min)	%MeOH	%H ₂ O
initial	1.1	65	35
5	1.1	65	35
30	1.1	75	25
40	1.1	100	0

Table 12: Method of Separation for Iodotoluenes

Time (min)	Flow Rate (mL/min)	%MeOH	%H ₂ O
initial	1.1	44	56
10	1.1	44	56
30	1.1	46	54
40	1.1	48	52
50	1.1	100	0

APPENDIX

Table 13 - Competitive Rate Experiment Data For Iodoanilines versus Iodobenzene

Time (hrs)	Peak Area		Peak Area		Ratio	Ratio
	<i>meta</i> -	H-	<i>para</i> -	H-	[<i>m</i>]/[H]	[<i>p</i>]/[H]
initial	11.8	30.1	34.8	7.67	1.02	1.01
0 TMS addition	2989	7934	28485	5944	0.59	1.07
0.5	5.74	25.7	29.9	2.54	1.00	2.63
1.0	26.8	6	32.3	2.79	1.00	2.58
1.5	25.4	5.68	30.7	2.62	1.00	2.62

Table 14 - Competitive Rate Experiment Data For Iodoanisoles versus Iodobenzene

Time (hrs)	Peak Area		Peak Area		Ratio	Ratio
	<i>meta</i> -	H-	<i>para</i> -	H-	[<i>m</i>]/[H]	[<i>p</i>]/[H]
initial	25.8	13	10.2	15.2	1.03	1.02
0 TMS addition	15.5	11.4	7.42	10.4	0.71	1.09
0.5	4.84	6.19	6.28	5.73	0.63	1.67
1.0	11.7	9.55	17.8	7.39	0.64	3.66
1.5	11.4	9.4	19.6	8.26	0.63	3.61
2.0	10.9	9.01	19.8	8.37	0.63	3.60
2.5	5.39	4.84	19.7	8.39	0.58	3.57

Table 15 - Competitive Rate Experiment Data For Iodobenzotrifluorides versus Iodobenzene

Time (hrs)	Peak Area		Peak Area		Ratio	Ratio
	<i>meta</i> -	H-	<i>para</i> -	H-	[<i>m</i>]/[H]	[<i>p</i>]/[H]
initial	40.5	47	40.8	11.7	0.99	1.04
0 TMS addition	14.5	8.42	22.8	7.98	1.98	0.86
0.5	10.1	8.53	0	9.02	1.36	0
1.0	8.54	8.44			1.16	
1.5	5	5.81			0.99	
2.0	5	7.61			0.76	
2.5	5	7.52			0.77	

Table 16 - Competitive Rate Experiment Data For Iodonitrobenzenes versus Iodobenzene

Time (hrs)	Peak Area		Peak Area		Ratio	Ratio
	<i>meta</i> -	H-	<i>para</i> -	H-	[<i>m</i>]/[H]	[<i>p</i>]/[H]
initial	31.5	7.28	23.9	8.13	1.02	1.03
0 TMS addition	9812	4628	12.3	7.53	0.50	0.57
0.5	0.131	5.96	0	5.33	0.01	0
1.0	0	5.35			0	

Table 17 - Competitive Rate Experiment Data For Iodophenols versus Iodobenzene

Time (hrs)	Peak Area		Peak Area		Ratio	Ratio
	<i>meta</i> -	H-	<i>para</i> -	H-	[<i>m</i>]/[H]	[<i>p</i>]/[H]
initial	14.3	15.8	18.6	10.1	1.01	1.01
0 TMS addition	12.7	14.2	19.2	9.22	1.00	1.14
0.5	9.65	8.24	18.5	2.65	1.32	3.82
1.0	9.29	7.73	19.1	2.75	1.35	3.80
1.5	10.2	8.34	19.1	2.59	1.37	4.03
2.0	9.3	7.63	19.2	2.69	1.37	3.90

Table 18 - Competitive Rate Experiment Data For Iodotoluenes versus Iodobenzene

Time (hrs)	Peak Area		Peak Area		Ratio	Ratio
	<i>meta</i> -	H-	<i>para</i> -	H-	[<i>m</i>]/[H]	[<i>p</i>]/[H]
initial	6308	6887	1439	1714	1.03	1.03
0 TMS addition	4880	5692	6837	6420	0.96	1.31
0.5	2.86	3.95	5.33	3.93	0.81	1.67
1.0	2.8	3.96	4.98	3.75	0.79	1.63
1.5	2.92	4.11	5.47	4.46	0.80	1.51
2.0			5.47	4.25		1.58
2.5			5.47	4.25		1.66

Table 19 - Competitive Rate Experiment Data For 4-Iodoethylbenzene versus Iodobenzene

Time (hrs)	Peak Area		Ratio
	<i>para</i> -	H-	[<i>p</i>]/[H]
initial	15.6	9.29	1.05
0 TMS addition	10229	6084	1.05
0.5	6.81	2.82	1.51
1.0	6.46	2.69	1.50
1.5	6.03	2.45	1.54

References

1. Saito, I; Nakatani, K. *Bull. Chem. Soc. Jpn.* **1996**, *69*, 3007.
2. Grissom, J. W.; Gunawardena, G. U.; Klingberg, D.; Huang, D. *Tetrahedron* **1996**, *52*, 6453.
3. Maier, M. E.; Abel, U. *Synlett* **1995**, 38.
4. Maier, M. E.; Boße, F.; Niestroj, A. J. *Eur. J. Org. Chem.* **1999**, 1.
5. Myers, A G.; Tom, N. J.; Fraley, M. E.; Cohen S. B.; Madar, D. J. *J. Am. Chem. Soc.* **1997**, *119*, 6072.
6. Shair, M. D.; Yoon, T.; Chou, T. -C.; Danishefsky, S. J. *Angew. Chem. Int. Ed. Engl.* **1994**, *33*, 2477.
7. Myers, A. G.; Kort, M. E.; Cohen, S. B.; Tom, N. J. *Biochemistry* **1997**, *36*, 3903.
8. Srinivasan, V.; Jebaratnam, D. J.; Budil, D. E. *J. Org. Chem.* **1999**, *64*, 5644.
9. Smith, A. L.; Nicolaou, K. C. *J. Med. Chem.* **1996**, *39*, 2103.
10. Dai, W. -M.; Lai, K. W.; Wu, A.; Hamaguchi, W.; Lee, M. Y. H.; Zhou, L.; Ishii, A.; Nishimoto, S. *J. Med. Chem.* **2002**, *45*, 758.
11. Evenzahav, A.; Turro, N.J. *J. Am. Chem. Soc.* **1998**, *120*, 1835.
12. Konig, B.; Pitsch, W. *J. Org. Chem.*, **1996**, *61*, 4258.
13. Konig, B. *Eur. J. Org. Chem.* **2000**, 381.
14. Turro, N.J.; Evenzahav, A.; Nicolaou, K.C. *Tetrahedron Lett.* **1994**, *35*, 8089.
15. Maier, M. E. *Synlett* **1995**, 13.
16. McHugh, M.M.; Yin, X.; Kuo, S. -R.; Liu, J.-S.; Melendy, T.; Beerman, T.A. *Biochemistry* **2001**, *40*, 4792.
17. Jones, R. R.; Bergman, R. G. *J. Am. Chem. Soc.* **1972**, *94*, 660.
18. Plourde, G.W.II; Warner, P. M.; Parrish, D. A.; Jones, G. B. *J. Org. Chem.* **2002**, *67*, 5369.
19. Bergman, R.G. *Acc. Chem. Res.* **1973**, *6*, 25.
20. Lockhart, T. P.; Bergman, R. G. *J. Am. Chem. Soc.* **1981**, *103*, 4091.

21. Maier, M. E.; Langenbacher, D. *Synlett* **1996**, 682.
22. Brana, M. F.; Moran, M.; de Vega, M. J. P.; Pita-Romero, I. *Tetrahedron Lett.* **1994**, *35*, 8655.
23. Nicolaou, K. C.; Dai, W. M.; Tsay, S. C.; Estevez, V. A.; Wrasidlo, W. *Science* **1992**, *256*, 1172.
24. Nicolaou, K.C.; Zuccarello, G.; Ogawa, Y.; Schweiger, E.J.; Kumazawa, T. *J. Am. Chem. Soc.* **1988**, *110*, 4866.
25. Snyder, J.P. *J. Am. Chem. Soc.* **1989**, *111*, 7630.
26. Magnus, P.; Fortt, S.; Pitterna, T.; Snyder, J.P. *J. Am. Chem. Soc.* **1990**, *112*, 4986.
27. Snyder, J.P. *J. Am. Chem. Soc.* **1990**, *112*, 5367.
28. Feldgus, S.; Shields, G.C. *Chem. Phys. Lett.* **2001**, *347*, 505.
29. Semmelhack, M.F.; Neu, T.; Foubelo, F. *Tetrahedron* **1992**, *33*, 3277.
30. Semmelhack, M.F.; Neu, T.; Foubelo, F. *J. Org. Chem* **1994**, *59*, 5038.
31. Myers, A.G.; Dragovich, P.S. *J. Am. Chem. Soc.* **1992**, *114*, 5859.
32. Kim, C.S.; Russell, K.C. *J. Org. Chem.* **1998**, *63*, 8229.
33. Nicolaou, K.C.; Ogawa, Y.; Zucarello, G.; Kataoka, H. *J. Am. Chem. Soc.* **1988**, *110*, 7247.
34. Kim, C.S.; Russell, K.C. *Tetrahedron* **1999**, *40*, 3835.
35. Choy, N.; Kim, C.S.; Ballestro, C.; Artigas, L.; Diez, C.; Lichtenberger, F.; Shapiro, J.; Russell, K.C. *Tetrahedron* **2000**, *41*, 6955.
36. Grissom, J.W.; Calkins, T.L.; McMillen, H.A.; Jiang, Y. *J. Org. Chem.* **1994**, *59*, 5833.
37. Rawat, D.S.; Zaleski, J.M. *J. Chem. Soc., Chem. Commun.* **2000**, 2493.
38. Jones, G.B.; Warner, P.M. *J. Am. Chem. Soc.* **2001**, *123*, 2134.
39. Konig, B.; Pitsch, W.; Klein, M.; Vasold, R.; Prall, M.; Schreiner, P.R. *J. Org. Chem.* **2001**, *66*, 1742.
40. Calvert, J. G.; Pitts, J. N. Jr. *Photochemistry*; John Wiley & Sons, Inc., New York, **1967**.
41. Clark, A.E.; Davidson, E.R.; Zaleski, J.M. *J. Am. Chem. Soc.* **2001**, *123*, 2650.

42. Jones, G.B.; Wright, J.M.; Plourde, G. II; Purohit, A.D.; Wyatt, J.K.; Hynd, G.; Fouad, F. *J. Am. Chem. Soc.* **2000**, *122*, 9872.
43. Choy, N.; Blanco, B.; Wen, J.; Krishan, A.; Russell, K. C. *Org. Lett.* **2000**, *2*, 3761.
44. Tilley, J.W.; Zawoiski, S. *J. Org. Chem.* **1988**, *53*, 386.
45. Amatore, C.; Jutand, A. *Acc. Chem. Res.* **2000**, *33*, 314.
46. Wu, J.; Liao, Y.; Yang, Z. *J. Org. Chem.* **2001**, *66*, 3642.
47. Nuss, J.M.; Murphy, M.M. *Tetrahedron* **1994**, *35*, 37.
48. Grissom, J.W.; Calkins, T.L.; McMillen, H.A. *J. Org. Chem.* **1993**, *58*, 6556.
49. Grissom, J.W.; Calkins, T.L.; Egan, M. *J. Am. Chem. Soc.* **1993**, *115*, 11744.
50. Chandra, T.; Pink, M.; Zaleski, J.M. *Inorg. Chem.* **2001**, *40*, 5878.
51. Rawat, D.S.; Zaleski, J.M. *J. Am. Chem. Soc.* **2001**, *123*, 9675.
52. Hopf, H.; Theurig, M. *Angew. Chem. Int. Ed. Engl.* **1994**, *33*, 1099.
53. Thorand, S.; Krause, N. *J. Org. Chem.* **1998**, *63*, 8551.
54. Huynh, C.; Linstrumelle, G. *Tetrahedron*, **1998**, *44*, 6337.
55. Stephen, R. D.; Castro, C. E. *J. Org. Chem.* **1963**, *28*, 3313.
56. Sonogashira, K.; Tohda, Y.; Hagihara, N. *Tetrahedron Lett.* **1975**, *33*, 4467.
57. Xu, J.; Egger, A.; Bernet, B.; Vasella, A. *Helvetica Chimia Acta* **1996**, *79*, 2004.
58. Sakai, Y.; Nishiwaki, E.; Shishido, K.; Shibuya, M.; Kido, M. *Tetrahedron Lett.* **1991**, *32*, 4363.
59. Grissom, J. W.; Klingberg, D.; Huang, D.; Slattery, B. J. *J. Org. Chem.* **1997**, *62*, 603.
60. Magnus, P.; Miknis, G. F.; Press, N. J.; Grandjean, D.; Taylor, G. M.; Harling, J. *J. Am. Chem. Soc.* **1997**, *119*, 6739.
61. Rao, P. D.; Littler, B. J.; Geier, R. III.; Lindsey, J. S. *J. Org. Chem.* **2000**, *65*, 1084.
62. Strachan, J-P.; O'Shea, D. F.; Balasuramanian, T.; Lindsey, J. S. *J. Org. Chem.* **2000**, *65*, 3160.

63. Gilow, H. M.; Burton, D. E. *J. Org. Chem.* **1981**, *46*, 2221.
64. Choi, D-S.; Huang, S.; Huang, M.; Barnard, T. S.; Adams, R. D.; Seminario, J. M.; Tour, J. M. *J. Org. Chem.* **1998**, *63*, 2646.
65. Chan, H-W.; Chan, P-C.; Liu, J-H.; Wong, H. N. C. *Chem. Commun.* **1997**, 1516.
66. Burzin, K.; Enderer, K. *Angew. Chem. Int. Ed.* **1972**, *11*, 151.
67. Jähnisch, K.; Weigt, E.; Bosies, E. *Synthesis*, **1992**, 1211.
68. Sakamoto, T; Shiraiwa, M; Kondo, Y; Yamanaka, H *Synthesis*, **1983**, 312.
69. Hammett, L.P. *J. Am. Chem. Soc.* **1937**, *59*, 96.
70. Andrea Aguirre, A reactivity and mechanistic study of the Sonogashira coupling and Grignard-Sonogashira coupling reactions , M.Sc. Thesis, Lakehead University, 2002.
71. McDaniel, D. H.; Brown, H. C. *J. Org. Chem.* **1958**, *23*, 420.
72. Kaiser, R. *Gas Phase Chromatography* Vol I, London, 1963.
73. Kaiser, R. *Gas Phase Chromatography* Vol II, London, 1963.
74. Havens, ; Hergenrother, *J. Org. Chem.* **1985**, *50*, 1763.